

---

# Entanglement and Its Applications in Systems with Many Degrees of Freedom

---

Stein Olav Skrøvseth

Thesis submitted in partial fulfillment of the requirements  
for the Norwegian academic degree philosophiæ doctor.

Department of Physics  
Norwegian University of Science and Technology  
Trondheim, Norway

December, 2006



# List of articles

## Paper I [SO05]

Stein Olav Skrøvseth and Kåre Olaussen,  
*Entanglement used to identify critical systems*,  
Phys. Rev. A, **72**, 022318 (2005) [cond-mat/0503235]

We promote use of the geometric entropy formula derived by Holzhey et. al. from conformal field theory,  $S_\ell \sim (c/3) \log(\sin \pi \ell / N)$ , to identify critical regions in zero temperature 1D quantum systems. The method is demonstrated on a class of one-dimensional  $XY$  and  $XYZ$  spin-1/2 chains, where the critical regions and their corresponding central charges can be reproduced with quite modest computational efforts.

## Paper II [Skr05a]

Stein Olav Skrøvseth,  
*Entanglement in bosonic systems*,  
Phys. Rev. A, **72**, 062305 (2005) [quant-ph/0508160]

We present a technique to resolve a Gaussian density matrix and its time evolution through known expectation values in position and momentum. Further we find the full spectrum of this density matrix and apply the technique to a chain of harmonic oscillators to find agreement with conformal field theory in this domain. We also observe that a non-conformal state has a divergent entanglement entropy.

## Paper III [Skr05b]

Stein Olav Skrøvseth,  
*Entanglement signatures in critical quantum systems* in  
Proceedings of ERATO conference on Quantum Information Science 2005, 177 (2005)

Conformal field theory (CFT) predicts a signature in the entanglement entropy of conformally invariant systems. These include critical quantum systems in 1+1 dimension with local interactions, and we present a technique to identify criticality in such system through this signature. It is shown that this detection is precise even in systems small enough to facilitate numerical diagonalization of the Hamiltonian.

**Paper IV [Skr06a]**

Stein Olav Skrøvseth,

*Entanglement properties of quantum spin chains,*

Phys. Rev. A, **74**, 022327 (2006) [quant-ph/0602233]

We investigate the entanglement properties of a finite size 1+1 dimensional Ising spin chain, and show how these properties scale and can be utilized to reconstruct the ground state wave function. Even at the critical point, few terms in a Schmidt decomposition contribute to the exact ground state, and to physical properties such as the entropy. Nevertheless the entanglement here is prominent due to the lower-lying states in the Schmidt decomposition.

**Paper V [Skr06b]**

Stein Olav Skrøvseth,

*Thermalization through unitary evolution of pure states,*

Europhys. Lett., **76**, 1179 (2006) [quant-ph/0606216]

The unitary time evolution of a critical quantum spin chain with an impurity is calculated, and the entanglement evolution is shown. Moreover, we show that the reduced density matrix of a part of the chain evolves such that the fidelity of its spectrum is very high with respect to a state in thermal equilibrium. Hence, a thermal state occurs through unitary time evolution in a simple spin chain with impurity.

# Acknowledgements

The writing of a PhD thesis is a vast and lonely task, and the present thesis is no exception in that respect. However, the work is made ever more inspiring with colleagues and friends around for discussion and support.

Professor Kåre Olaussen has been an indispensable resource in the work of this thesis with his great insight into numerous and varied areas of physics. His sociable and friendly personality has made it a true pleasure to work with him.

I am grateful that Professors José Ignacio Latorre, Henrik Johannesson, and Johannes Skaar have agreed to constitute the evaluating committee for the present thesis and the defense to be held on December 12, 2006.

My fellow students at NTNU have provided a great network for inspiring coffee breaks and physics discussions. Great credit is given to Jo Smiseth, Martin Grønsleth, Jan Petter Morten, Kjetil Børkje, Daniel Huertas-Hernando, and Jan Øystein Haavik Bakke for their inspiration, and for providing a great atmosphere in the physics department. Martin, Jan Petter and Kjetil are also thanked for proofreading parts of the thesis.

The NordForsk network on Low-dimensional Physics administered by Susanne Viefers is acknowledged for arranging inspiring meetings, and economic support. Stephen Bartlett in Sydney is thanked for providing a great opportunity to go to Australia at the end of this work.

The final years of the PhD work has been spent at the world's northernmost university, the University of Tromsø. I would like to thank Robert Jenssen, Eivind Brodahl, Tor Arne Øigård, and Stian Anfinssen for making me feel most welcome, even though their scientific interests are at best tangential to the present work.

Parental support is indispensable, and in this case it has always been good to know that I am welcome at my childhood home when coming back to Trondheim, thanks to my parents and brother.

My deepest gratitude goes to my beloved Veronika Kristine Tømmerås, who has always been supportive and loving, and whose company and inspiration has been fantastic through these years.

Finally, I cannot overestimate the inspiration provided by the creativity and great friendship of Bendik Kvale Jacobsen.



# Table of Contents

<b>1</b>	<b>Introduction</b>	<b>1</b>
<b>2</b>	<b>Entanglement</b>	<b>5</b>
2.1	Entanglement measures . . . . .	7
2.1.1	Forming and distilling entanglement . . . . .	8
2.1.2	Concurrence . . . . .	10
2.1.3	Other entanglement measures . . . . .	11
2.1.4	Rényi entropy . . . . .	12
2.2	Entanglement in quantum information . . . . .	12
<b>3</b>	<b>Numerical Analysis</b>	<b>15</b>
3.1	Using symmetries . . . . .	16
3.2	Renormalization techniques . . . . .	19
<b>4</b>	<b>Continuous Variables</b>	<b>21</b>
4.1	Weyl algebra . . . . .	22
4.2	Gaussian states . . . . .	23
4.3	The Klein-Gordon field . . . . .	25
4.4	Two-mode entanglement . . . . .	26
4.5	State evolution . . . . .	27
<b>5</b>	<b>Quantum Critical Systems</b>	<b>31</b>
5.1	Ground state entropy . . . . .	33
5.2	Consequences of conformal symmetry . . . . .	33
5.2.1	The free boson . . . . .	36

5.2.2	The free fermion . . . . .	37
5.2.3	Entanglement entropy in a $1 + 1$ dimensional strip . . . . .	37
5.2.4	Conformal invariance in QPT . . . . .	39
5.3	Quantum models . . . . .	40
5.3.1	The Ising model . . . . .	41
5.3.2	The $XX$ model . . . . .	43
5.4	The $XY$ model . . . . .	44
5.4.1	Fermionization . . . . .	45
5.4.2	Diagonalization in terms of Majorana fermions . . . . .	48
5.4.3	Entropy in the $XY$ model . . . . .	52
5.4.4	Other correlators . . . . .	54
5.4.5	Determining criticality . . . . .	55
5.5	Criticality in the $XYZ$ model . . . . .	57
5.5.1	Critical surfaces . . . . .	57
5.6	Time evolution . . . . .	59
5.7	The quantum Hall effects . . . . .	61
5.7.1	FQHE on a torus . . . . .	63
5.7.2	Entanglement in the FQHE . . . . .	64



# List of Figures

1.1	A physical implementation of “Bob”. . . . .	2
2.1	The binary entropy function . . . . .	9
2.2	Conceptual sketch of entropy and concurrence. . . . .	11
3.1	The reduction in complexity when utilizing symmetries. . . . .	18
4.1	Two-mode Gaussian entanglement in the Klein-Gordon field . . . . .	28
4.2	Field expectation values with time in a bosonic field with impurity . . . . .	29
5.1	Phase diagram for a quantum phase transition . . . . .	32
5.2	Conformal transformations in $1 + 1$ dimensions. . . . .	39
5.3	The gap in the Ising model. . . . .	42
5.4	Phase diagram of the $XY$ model . . . . .	45
5.5	The energy modes for various places in the $XY$ model. . . . .	48
5.6	The parity of the ground state in the $XY$ model. . . . .	49
5.7	Entropy of the $XY$ model. . . . .	53
5.8	Correlation length in the Ising model . . . . .	54
5.9	Illustration of the technique to find a critical line. . . . .	56
5.10	The critical region of the $XYZ$ model with $\gamma = 0$ . . . . .	57
5.11	Critical lines of the $XYZ$ model with $c = 1/2$ . . . . .	58
5.12	Experimental setup and data for the fractional quantum Hall effect. . . . .	61



---

# 1 Introduction

---

Erwin Schrödinger called entanglement the characteristic trait of quantum mechanics, the single concept that stands out not to have any counterpart in classical physics. Richard Feynman said that there is only one mystery in quantum mechanics, and that is entanglement and the consequences thereof. Albert Einstein was – along with many of his contemporaries – uncomfortable with what he called “spooky action at a distance”, and co-wrote the seminal paper [EPR35] where the authors dismissed the idea that quantum mechanics could possibly be a complete description of Nature on the grounds that it contained entanglement. Today entanglement is accepted as a trait of Nature, and though many aspects are poorly understood, the idea of a quantum computer has shifted much of the research away from fundamental investigation to pragmatical work on how to utilize entanglement in quantum computing and quantum communication [NC00].

Entanglement is essentially a question of correlations. Correlations are a well known daily life phenomenon. We all know that wearing a seat belt is correlated with our chances of avoiding serious injury in a car accident. Other correlations are less obvious, and are often the focus of research, e.g. whether there is a correlation between the CO<sub>2</sub> content in the atmosphere and global warming, whether there is a correlation between certain diets and the risk of acquiring cancer, or how correlated the number of years of education is with income. In classical theories a correlation can never be better than perfect, the best we can do is a perfect correlation, e.g. if a certain number of years in school linearly increases the yearly income. As all scientists know, this is not the case, but probably there is a less than perfect, though positive correlation. However, quantum mechanics opens the case that there might be better than perfect correlations. This is the case when considering e.g. the spin of two electrons separated by some spatial distance. We can measure the spin of one, and it may not only be correlated with what we measure on the other electron, but it will be more than 100% correlated; the electrons were *entangled* before the measurement. In the simplistic case described here, this will never be evident, all we can see in our measurements is a perfect correlation. However, John Bell wrote down an inequality in

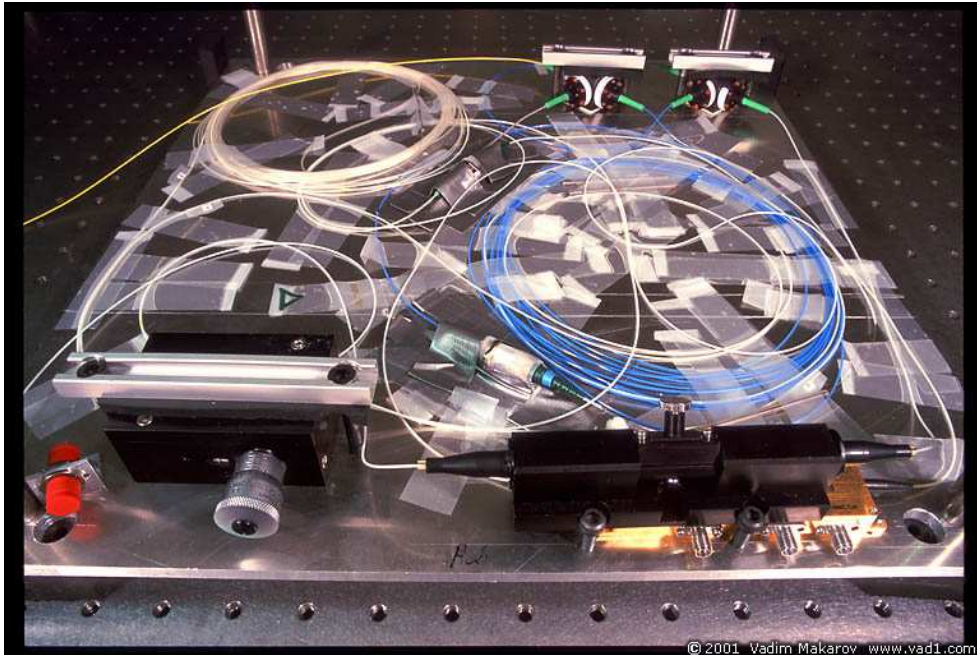


**Figure 1.1:** A physical implementation of “Bob”, one of the characters of quantum information theory. This is the setup used in an optical quantum cryptography experiment at the Department of Electronics and Telecommunications, NTNU. Image courtesy of Vadim Makarov, used with permission.

1964 [Bel64] that would be satisfied for all classical correlations, but would possibly be broken if there were quantum correlations present. Now it is accepted as an experimental fact that Bell’s inequality may be broken, as first confidently demonstrated by Alain Aspect *et al.* in 1982 [ADR82]. Thus Nature seems to allow quantum correlations on top of the classical correlations. This excess correlation is what we know as entanglement, and is evident whenever Bell’s inequality is broken.

Though the connection is not obvious, entanglement is today mainly studied in connection with quantum information theory, as it is believed that a quantum computer will – if ever built – utilize entanglement to perform certain computational tasks faster than classically possible. Feynman pointed out in 1982 that simulating quantum systems on a classical computer was nearly impossible due to the much larger Hilbert space of the quantum variant [Fey82]. Thus, he suggested the use of a quantum computer to simulate quantum systems. However, it was not until Peter Shor’s discovery in 1994 [Sho94] that a quantum computer could factorize large numbers exponentially faster than classically possible that the idea really gained momentum. The quantum computer is still very much a theoretical device, despite considerable experimental effort on small scale systems. It has so far not emerged any single clear candidate for the implementation of the quantum bits (qubits) and the operations needed to process the quantum information. The NMR experiment that factorized the number 15 in 2001 [VSB<sup>+</sup>01] was the first implementation where a

quantum algorithm was proved to work, though on a relatively trivial problem. The NMR implementation, along with most implementations based on atomic, molecular or optical physics (AMO), is poorly scalable. The approach based on ion traps has nevertheless become fashionable, and was one of the first promising proposals for a quantum computer made in 1995 by Cirac and Zoller [CZ95]. Other implementations are based on condensed matter systems, such as superconducting qubits or quantum dots. The main problem in many of these approaches is decoherence, that is the qubits become entangled with the environment and thus information is lost into the environment during the computation. Recently, two superconducting qubits were entangled [SAB<sup>+</sup>06], making it an ever more promising candidate for quantum computing. Also recently, a hybrid approach has been proposed, exploiting the advantages of different schemes [ADD<sup>+</sup>06], where trapped polar molecules are controlled by a microwave field set up by running superconductors. Despite the extensive effort, one still doesn't know whether the quantum computer even can be built, or if one might encounter a fundamental reason why this is an impossible feat. Even so, the process will learn us fundamental facts about physics and the process cannot be said to have been in vain.

Phase transitions are also familiar phenomena of daily life, like the freezing of water at zero temperature. Such classical phase transitions occur when the temperature is changed across some critical value  $T_c$ , and the thermal fluctuations are exactly what drives the system from one thermodynamical state to another. Quantum phase transitions on the contrary, can happen at zero temperature, and therefore without thermal fluctuations. These continuous phase transitions occur when the ground state changes nature through the variation of a parameter, such as an external magnetic field. The only fluctuations present are the quantum fluctuations that must exist due to the Heisenberg uncertainty relation, and hence the name quantum phase transitions. The wave function of the system at the critical point is very complicated, as is evident from the fact that it carries more entanglement than at off-critical points. The complexity of the wave function at the critical point also means that more information is encoded in the wave function, thus making it more usable for quantum information.

This thesis is organized as follows; Chapter 2 is a brief introduction to the most important principles in entanglement theory, with an emphasis on those subjects which are considered in later chapters. Chapter 3 addresses some general issues when it comes to modelling quantum systems on a classical computer, and the line is drawn between renormalization schemes and the problem of finding the ground state of a quantum system as addressed in [Skr06a]. In Chapter 4 we investigate bosonic systems, and compute the entanglement therein. In particular, the results from [Skr05a] are connected to other results from the theory of entanglement in continuous variable systems. Finally, Chapter 5 contains the bulk part of the thesis, summarizes quantum critical systems, and applies ideas from [SO05, Skr05b, Skr06a, Skr06b].

In all chapters, unless otherwise specified, units such that  $\hbar = c = 1$  are used, where  $c$  is

the speed of light in vacuum. All notation is as far as possible applied as is conventional in the literature. In particular, the symbol  $\oplus$  is used for the direct sum of matrices, e.g.  $A \oplus B = \text{diag}(A, B)$ , while  $\otimes$  designates direct product, which for matrices is defined in e.g. [NC00].

---

## 2 Entanglement

---

In its simplest form, entanglement arises from the possibility opened by quantum theory to write down a wave function that is non-local, encompassing two constituents separated by arbitrarily large distances. Consider a wave function of two particles shared by the protagonists of quantum information theory, Alice and Bob. Now, any measurement on either's part implies the collapse of the wave function at the other's side. This collapse happens instantly (in some frame of reference), and this is the source to its counter-intuitivity, not to mention the apparent contradiction with special relativity. However, Alice and Bob can never exploit this effect to communicate any information faster than the speed of light. Due to the statistical nature of the outcomes, the parties need to communicate classically to compare their results. Moreover, the simple scheme here can easily be explained through classical means with some "hidden variable" interpretation. However, there are more complicated schemes that efficiently demonstrate the breaking of Bell-type inequalities, thus ruling out any hidden variable explanation [Mer85]. In this thesis we will restrict our investigation to bipartite entanglement, and ignore the case where there are more parties than Alice and Bob. Thus, consider two systems in separate Hilbert spaces  $\mathcal{H}_A$  and  $\mathcal{H}_B$  respectively. Given a state vector  $|\psi\rangle_A \in \mathcal{H}_A$  in the first system and a state vector  $|\varphi\rangle_B \in \mathcal{H}_B$  in the second, we can define a state in the entire Hilbert space,  $\mathcal{H} = \mathcal{H}_A \otimes \mathcal{H}_B$  as

$$|\Psi\rangle_{\text{separable}} = |\psi\rangle_A \otimes |\varphi\rangle_B.$$

As indicated, this is a separable state, and any state that can be written in this way is separable, and thus carries no entanglement. More generally, the state of the entire system can be written as a Schmidt decomposition

$$|\Psi\rangle = \sum_{i=1}^{\chi} \sqrt{\lambda_i} |\psi_i\rangle_A \otimes |\varphi_i\rangle_B \quad (2.1)$$

where the upper limit of the sum,  $\chi$ , is called the Schmidt number of the state, and is maximally equal to the *smallest* of the dimensionalities of the two Hilbert spaces in

question. The states  $|\psi_i\rangle$  are orthogonal for all  $i$ , and the same is true for  $|\varphi_i\rangle$ . The expansion is unique, and the Schmidt number can be considered a very brute measure of entanglement, in particular the measure  $E(|\Psi\rangle) = \log_2 \chi$  fulfills some of the requirements for an entanglement measure as described later [Vid03].

Identifying an entangled state can, as opposed to what impression one gets from the simple analysis above, be a very hard task. The problem can be stated as finding the basis in which one can write a given state as a separable one, or proving that no such basis exists. It is important to realise that this task depends heavily on the choice of partitioning of the system. The task of writing down this basis indeed seems so daunting that one often resorts to simply stating whether a state is separable or not, and if it is non-separable, how much entanglement do we have? We will return to this problem in Section 2.1.

Given a Schmidt decomposition of a pure state  $|\Psi\rangle$ , one can straightforwardly write down the density matrix of (say)  $\mathcal{H}_A$  as

$$\rho^{(A)} = \sum_i \lambda_i |\psi_i\rangle\langle\psi_i|$$

where we have omitted the index  $A$  since the identity of the Hilbert space is obvious. This density matrix contains all information accessible to Alice. Hence, finding the Schmidt decomposition of the pure state wave function is equivalent to diagonalizing the reduced density matrices of the two subspaces. That is one indication of the importance of the Schmidt decomposition.

More generally though, the state in the full Hilbert space  $\mathcal{H}$  may not be a pure one, but an indeterminate mixed state with density matrix  $\rho$ . Still, the reduced density matrix of  $\mathcal{H}_A$  is well defined, but the entanglement is not, in the sense that one cannot find a genuine measure of entanglement for the state. Purification learns us that any mixed state in a Hilbert space  $\mathcal{H}$  can always be interpreted as a pure state in some (imaginary) larger Hilbert space  $\mathcal{H}' \supset \mathcal{H}$ . Consequently, the physical state  $\rho \in \mathcal{H}$  is entangled to the system of the larger Hilbert space  $\mathcal{H}'$ .

If Alice has access to the pure states  $\{\rho_i^{(A)}\} \in \mathcal{H}_A$  and Bob has the pure states  $\{\rho_i^{(B)}\} \in \mathcal{H}_B$ , the state

$$\rho = \sum_{ij} p_{ij} \rho_i^{(A)} \otimes \rho_j^{(B)} \quad \sum_{ij} p_{ij} = 1$$

carries only classical correlations, and must thus be classified as unentangled, or separable [Wer89]. A density matrix that is non-separable consequently is entangled, but finding a decomposition for a given density matrix is computationally hard. Moreover, for the case where  $\rho$  is a mixed state, it is not yet known how to measure the entanglement of the state such that classical correlations are eliminated.

Assume Alice and Bob being at different locations, separated by a large distance, and sharing a state describe by the density matrix  $\rho$ . Now, each party may operate on their state



by unitary transformations or measurements, and they are even allowed to communicate classically, e.g. through telephone, but any joint operation on both parties are prohibited. This protocol is known as LOCC, Local Operations and Classical Communication. Through LOCC one can generate all classical correlations, but no entanglement can ever be created this way. This means that LOCC describes the fundamental difference between what can be created classically and quantum mechanically and is a useful starting point to describe quantum correlations. What is sometimes called the fundamental law of quantum information processing can be phrased as

Through LOCC alone, Alice and Bob cannot increase the total entanglement of the state they share.

Mathematically, local operations can be either unitary operators  $U_A \in \mathcal{H}_A$  and  $U_B \in \mathcal{H}_B$  or general measurements  $\{\hat{A}_i\}$  and  $\{\hat{B}_i\}$ . The generalized measurements are complete, in the sense that

$$\sum_i \hat{A}_i^\dagger \hat{A}_i = \sum_i \hat{B}_i^\dagger \hat{B}_i = \mathbf{1},$$

where  $\hat{A}_i$  are measurements performed exclusively on Alice's system, and  $\hat{B}_i$  are performed on Bob's. After Alice has applied a measurement on her state  $\rho^{(A)}$ , the state collapses into  $\rho' = \hat{A}_i \rho^{(A)} \hat{A}_i^\dagger / p(i)$  with probability  $p(i) = \text{Tr}(\hat{A}_i \rho^{(A)} \hat{A}_i^\dagger)$ , and correspondingly for Bob's measurements. LOCCs are important in the sense that it should be assumed that entanglement cannot increase under LOCC, and should be invariant if there are no measurements involved.

Moreover, a fundamental fact involving LOCC is that, given two states  $|\psi_1\rangle$  and  $|\psi_2\rangle$ , of the joint system of Alice and Bob, one can transform the first into the latter by LOCC only if the ordered eigenvalues  $\lambda_1$  of  $\rho_1^{(A)} = \text{Tr}_B |\psi_1\rangle\langle\psi_1|$  is majorized by the eigenvalues  $\lambda_2$  of  $\rho_2^{(A)} = \text{Tr}_B |\psi_2\rangle\langle\psi_2|$ . A decreasingly ordered vector  $\vec{v}$  majorizes another ordered sequence  $\vec{w}$ , written  $v \succ w$  if

$$\sum_{i=1}^k v_i \geq \sum_{i=1}^k w_i \quad \text{for all } k = 1, \dots, d$$

where  $d$  is the smallest of the dimensions of the two vectors.

## 2.1 Entanglement measures

As we have pointed out, entanglement is very much considered a fundamental resource in nature, much like energy or information are considered resources in other contexts. And anything called a resource must be measured, so we would have some idea about how

“much” we have of that resource. Thus one needs to define entanglement measures, a very non-trivial task [Myh04]. For some state described by the density matrix  $\rho$ , we want the entanglement  $E(\rho) \in \mathbb{R}$  of the state. This measure must fulfill some basic requirements to be physically reasonable [VPRK97, HHH00];

- E1  $E(\rho) \geq 0$  with equality if  $\rho$  is separable.
- E2  $E(\rho) = E(U_A \otimes U_B \rho U_A^\dagger \otimes U_B^\dagger)$  where  $U_A$  and  $U_B$  are any local unitary operators on Hilbert spaces  $\mathcal{H}_A$  and  $\mathcal{H}_B$  respectively.
- E3 The entanglement cannot increase under LOCC,  $E(\Theta\rho) \leq E(\rho)$  where  $\Theta$  is any LOCC operator.
- E4 Convexity:  $\sum_i p_i E(\rho_i) \geq E(\sum_i p_i \rho_i)$ .
- E5 Partial additivity:  $E(\rho^{\otimes n}) = nE(\rho)$ .
- E6 Continuity: If  $\lim_{n \rightarrow \infty} \langle \psi^{\otimes n} | \rho_n | \psi^{\otimes n} \rangle = 1$  with  $\rho_n$  a density matrix of  $n$  pairs, then

$$\lim_{n \rightarrow \infty} \frac{1}{n} [E(|\psi\rangle\langle\psi|^{\otimes n}) - E(\rho_n)] = 0$$

One also often requires the normalization that the Bell state  $|\beta\rangle = (|00\rangle + |11\rangle)/\sqrt{2}$  should have unit entanglement. Any entanglement measure that satisfies conditions E1-4 is known as an *entanglement monotone*.

### 2.1.1 Forming and distilling entanglement

Given some quantum state  $\rho$ , the question of how much entanglement this contains is nontrivial. However, conceptually the question can be simplified by defining entanglement of formation and -distillation. Assume that we have a large number of Bell states, and are allowed to use only LOCC on these states, how many copies of a given bipartite state  $\rho$  can we make? The number of copies of  $\rho$  divided by the number of Bell states is known as the entanglement of formation  $E_F$  when one takes the limit of an infinite number of Bell states. On the contrary, the entanglement of distillation is defined as the number of Bell states we can create from a large number of copies of  $\rho$ . The distillable entanglement  $E_D$  is always less than or equal to the entanglement of formation since one inevitably loses information in the process of formation and distillation. Moreover, it turns out that any reasonable entanglement measure is bounded by these, [HHH00]

$$E_D(\rho) \leq E(\rho) \leq E_F(\rho). \tag{2.2}$$

For the special case of  $\rho = |\psi\rangle\langle\psi|$  being a pure state, it turns out that one can uniquely define a bipartite entanglement measure since the entanglement of formation and -distillation

are equal and equal to the von Neumann entropy of the reduced density matrix of one of the parties. That is,

$$E_F(|\psi\rangle\langle\psi|) = S(\rho') = -\text{Tr} \rho' \log_2 \rho' \quad \text{with} \quad \rho' = \text{Tr}_B |\psi\rangle\langle\psi| \quad (2.3)$$

where  $\rho'$  is the reduced density matrix accessible to Alice. The entanglement must be symmetric, so it does not matter whether we trace out Alice's or Bob's system. The von Neumann entropy is nothing but the Shannon entropy of the eigenvalues of the reduced density matrix, as the Shannon entropy of some random variable  $X$  with probabilities  $x_1, \dots, x_N$  is  $H(X) = -\sum_n x_n \log_2 x_n$ . Note that we use logarithm base two, meaning that the von Neumann entropy is measured in ebits (entanglement bits), and the von Neumann entropy of a shared Bell state is unity.

Consider the von Neumann entropy in the case of a single qubit, that is the density matrix

$$\rho = \alpha|0\rangle\langle 0| + \beta|0\rangle\langle 1| + \beta^*|1\rangle\langle 0| + (1 - \alpha)|1\rangle\langle 1| = \begin{bmatrix} \alpha & \beta \\ \beta^* & 1 - \alpha \end{bmatrix}.$$

This has two eigenvalues  $\lambda$  and  $1 - \lambda$ , and thus the von Neumann entropy becomes

$$S(\rho) = -\lambda \log_2 \lambda - (1 - \lambda) \log_2(1 - \lambda) \equiv H(\lambda), \quad (2.4)$$

which is known as the binary entropy function, shown in Figure 2.1.  $H(\lambda)$  is zero when  $\lambda = 0, 1$  and reaches maximum at  $\lambda = 1/2$  as  $H(1/2) = 1$ . Obviously, the former is a pure state, while the latter is a maximally entangled state for a single qubit.

For a general mixed state, the situation is more complicated. Indeed, it is very hard to eliminate the classical correlations in a mixed state such that the entanglement measure contains only the quantum correlations. The entanglement of formation for a mixed state

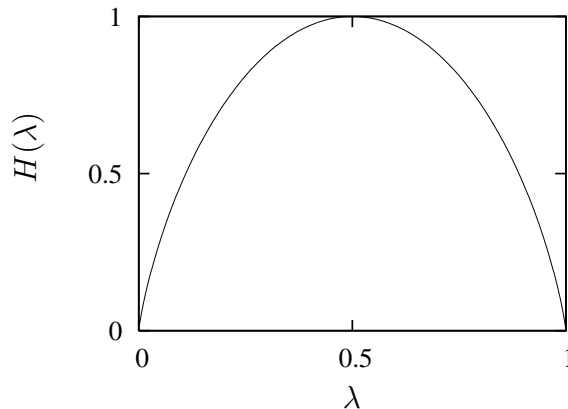


**Figure 2.1:** The binary entropy function  $H(\lambda) = -\lambda \log_2 \lambda - (1 - \lambda) \log_2(1 - \lambda)$ , which is the entanglement of a single qubit whose density matrix has eigenvalues  $\lambda$  and  $1 - \lambda$ .

$\rho$  is defined as

$$E_F(\rho) = \inf \left\{ \sum_k \lambda_k S(|\psi_k\rangle\langle\psi_k|) \mid \rho = \sum_k \lambda_k |\psi_k\rangle\langle\psi_k| \right\} \quad (2.5)$$

where the infimum is to be taken over all decompositions of  $\rho$  into pure states. Here,  $S(|\psi\rangle\langle\psi|)$  indicates the von Neumann entropy of (say) Alice's reduced density matrix  $\rho' = \text{Tr}_B |\psi\rangle\langle\psi|$ . The explicit computation of the entanglement of formation is known only for a limited number of cases, such as for the two-spin entanglement known as concurrence reviewed next, and the two-mode Gaussian entanglement reviewed in section 4.4.

### 2.1.2 Concurrence

Concurrence is a measure of entanglement in a system consisting of two spins, or any other two-level system that is closely related to the entanglement of formation [HW97, Woo98]. We consider a mixed state  $\rho$ , such as the reduced density matrix of two spins in a larger spin chain. The spin-flip operator on a qubit is defined as  $|\tilde{\psi}\rangle = \sigma^y |\psi^*\rangle$ , which flips the spin in the standard basis. Note that complex conjugation, like transposition, is a basis-dependent transformation and it is thus not a physical operation. Now, to flip both spins in the standard basis  $\{|\uparrow\uparrow\rangle, |\uparrow\downarrow\rangle, |\downarrow\uparrow\rangle, |\downarrow\downarrow\rangle\}$  take the transformed density matrix

$$\tilde{\rho} = (\sigma^y \otimes \sigma^y) \rho^* (\sigma^y \otimes \sigma^y),$$

and define the Hermitian matrix  $R = \sqrt{\rho^{1/2} \tilde{\rho} \rho^{1/2}}$  whose decreasingly ordered eigenvalues we denote  $\lambda_1 \geq \lambda_2 \geq \lambda_3 \geq \lambda_4$ , and assume that at least two of them are non-zero. The trace of  $R$  is simply the fidelity between the spin-flipped density matrix and the original<sup>1</sup>. Now the concurrence is defined as

$$C(\rho) = \max(0, \lambda_1 - \lambda_2 - \lambda_3 - \lambda_4). \quad (2.6)$$

The concurrence is a valid entanglement measure in its own right, but the entanglement of formation equals

$$E_F(\rho) = H \left( \frac{1}{2} \left[ 1 + \sqrt{1 - C(\rho)^2} \right] \right), \quad (2.7)$$

where  $H(x)$  is the binary entropy function (2.4). Since  $E_F(\rho)$  is a monotonically increasing function of  $C(\rho)$  and they coincide at zero and unity, they can be considered equivalent entanglement measures, and one usually call the concurrence simply the entanglement of formation due to this equivalence.

A conceptual sketch of the different ways to measure entanglement by concurrence and entanglement entropy is shown in Figure 2.2. The key point is that the entropy measures

<sup>1</sup>The fidelity is a distance measure between two quantum states, being unity if they are equal, and less than one, though positive, else. The fidelity is revisited in Section 5.6.

the entanglement of a set of (not necessarily contiguous) spins with the rest of the chain, where the whole chain is in a pure state. The concurrence, however measures the entanglement shared between only two spins, where these two spins together might be in a mixed state.

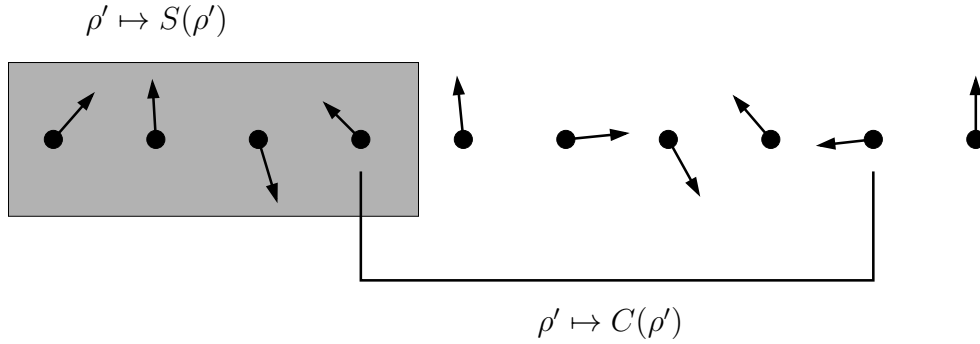


**Figure 2.2:** Conceptual sketch of the two entanglement measures entanglement entropy and concurrence in a spin chain. The former amounts to finding the reduced density matrix of a part of the spin chain and hence the entropy  $S(\rho) = -\text{Tr} \rho \log_2 \rho$ , while the second considers two individual spins in the chain and their entanglement is measured by the concurrence.

### 2.1.3 Other entanglement measures

There is a number of other measures of entanglement for mixed states that are entanglement monotones, most of which reduce to the entanglement entropy when one considers pure states. These include negativity, which is defined on a 2-qubit state as  $\mathcal{N}(\rho) = 2 \max(0, -\lambda_{\text{neg}})$  where  $\lambda_{\text{neg}}$  is the sum of the negative eigenvalues of  $\rho^{\text{T}B}$  where one takes the partial transpose of Bob's part of the density matrix [VW02].

Another measure that has gained attention recently is *squashed entanglement* or *conditional mutual information* (CMI) [CW04], which is defined as

$$E_{\text{CMI}}(\rho_{AB}) = \frac{1}{2} \inf_{\rho_{ABC}} S(A : B|C)$$

where the infimum is to be taken over all tripartite states that are such that  $\rho_{AB} = \text{Tr}_C \rho_{ABC}$ . The entropy  $S(A : B|C)$  is known classically as conditional mutual information and is the mutual information of  $A$  and  $B$  given  $C$ . Mutual information is given by

$$S(A : B) = S(\rho_A) + S(\rho_B) - S(\rho_{AB}),$$

while conditional mutual information is

$$S(A : B|C) = S(\rho_C) - S(\rho_{AC}) - S(\rho_{BC}) + S(\rho_{ABC}).$$

That is, we introduce an artificial system  $C$ , and compute the maximal information content in  $A$  and  $B$  given this system. Squashed entanglement is known to fulfill many of the requirements for entanglement measures and is a promising candidate for the final measure of entanglement for mixed states. However, the definition includes an extremalization that may be computationally very hard, though little has been done on computing squashed entanglement [Chr06].

### 2.1.4 Rényi entropy

The entanglement entropy (2.3) is not the only entropy one can define given the density matrix  $\rho$ , whose eigenvalues are  $\lambda_i$ . In particular, the von Neumann entropy is a special case of the Rényi entropy,

$$H_\alpha(\rho) = \frac{1}{1-\alpha} \log_2 \left( \sum_i \lambda_i^\alpha \right), \quad (2.8)$$

since  $S(\rho) = \lim_{\alpha \rightarrow 1} H_\alpha(\rho)$ . The Rényi entropy in a classical context where the eigenvalue spectrum is replaced by a probability distribution, has applications in several areas of physics and information theory, e.g. in signal processing [Jen05], along with the Shannon entropy, which is the classical equivalent of the von Neumann entropy. All Rényi entropies are zero if and only if  $\rho$  is a pure state and positive otherwise. Finally, in the limit  $\alpha \rightarrow \infty$  the Rényi entropy is simply the logarithm of the largest eigenvalue,

$$H_\infty(\rho) = -\log_2 \max_i \lambda_i. \quad (2.9)$$

This is known as the single-copy entanglement [EC05], since it measures how much entanglement can be extracted from a single specimen of  $\rho$ , rather than the asymptotic notion used to define entanglement of formation that leads to the von Neumann entropy.

## 2.2 Entanglement in quantum information

Entanglement is an important subject in its own right, as it challenges our understanding of Nature and how it works, and might be at the heart of physics. Nevertheless, it is in quantum information theory that applications of entanglement are known, and hence where the subject has gained the most attention. Shor's algorithm is an example of a quantum algorithm that utilizes entanglement as a computational resource. However, entanglement is not necessary for quantum computation, e.g. Grover's search algorithm does not attain its power from entanglement [Llo99]. This might be the reason that Grover's algorithm is a mere quadratic speedup, compared to Shor's exponential speedup relative to known classical algorithms.

Also, entanglement can be used as a resource in quantum communication, including superdense coding, where two classical bits can be transmitted by one qubit given that Alice and Bob share an entangled state before the communication [BW92]. Quantum teleportation [BBC<sup>+</sup>93] exploits a shared entangled state to transmit an arbitrary quantum state from Alice to Bob using only LOCC, a technique that has been experimentally implemented in atomic systems to much popular interest [KE04]. The quantum cryptography scheme due to Ekert also relies on distribution of entangled particles [Eke91], though the popular BB84 protocol does not use entanglement [BB84].





---

## 3 Numerical Analysis

---

The study of quantum mechanical systems that involve more than a few particles inevitably requires the use of classical computers to solve the system. The size of the Hilbert space of a system of  $N$  qubits increases exponentially as  $2^N$ , which is a contributing factor that a quantum computer may attain its vast computational power, but also naturally hampers simulations of quantum systems on a classical computer. And as long as we don't have the quantum computer, the simulations must be done on the classical variant. Given a quantum system of  $N$  spin-1/2 particles, a possible encoding of the qubit, a separable state is

$$|\psi_{\text{sep}}\rangle = \bigotimes_{n=1}^N (\alpha_n|0\rangle_n + \beta_n|1\rangle_n) \quad (3.1)$$

with  $\alpha_n$  and  $\beta_n$  complex coefficients. This gives  $2N$  degrees of freedom — overall phase factors and normalization corrected for. However, a general state is

$$|\psi\rangle = \sum_{\eta=0}^{2^N-1} \alpha_\eta |\eta\rangle$$

where  $|\eta\rangle$  are the orthogonal basis states, and  $\sum_\eta |\alpha_\eta|^2 = 1$ . The  $\alpha$ s now constitute  $2^N - 2$  degrees of freedom. Hence, when entanglement is not included, the complexity in the state is dramatically reduced as opposed to the general entangled state, although the schematic overview here is somewhat simplified.

It is also immediately clear that if one computes the spin-spin correlation function

$$\Gamma_{ij} = \langle \sigma_i^\alpha \sigma_j^\beta \rangle - \langle \sigma_i^\alpha \rangle \langle \sigma_j^\beta \rangle$$

for the separable state (3.1), it is identically zero. Hence, if there are any correlations in the state, they must arise from entanglement unless there are degeneracies or finite temperature, which means we may not have a pure state. It is a well-known fact from critical

phenomena that the correlation function decays exponentially with inter-spin distance,  $\Gamma_{ij} \sim e^{-|i-j|/\xi}$  for large distances,  $|i-j| \gg 1$ .  $\xi$  is then known as the correlation length. However, at critical points, the correlation function decays polynomially, thus demonstrating the fact that entanglement is much more prevalent at critical points than elsewhere in the parameter space.

Sometimes it is possible to map the system of interacting qubits onto a simpler system where the degrees of freedom grows linearly as opposed to exponentially, as we will explore in later chapters. However, this is not always possible, and much attention has been drawn to the subject of finding numerical recipes that can be used to efficiently compute e.g. the ground state of a Hamiltonian.

### 3.1 Using symmetries

Most models exhibit symmetries, that is operators that commute with the Hamiltonian, and thus share a common eigenvalue set with this. Imposing periodic boundary conditions on a model will lead to translational invariance, and thus conservation of momentum according to Noether's theorem. Thus, the full Hilbert space of the Hamiltonian can be reduced into subspaces with definite momenta, and thereby somewhat reducing the size of the matrices that one needs to diagonalize. This is not as efficient as other methods — by a long shot — but it may reduce the complexity enough to allow numerical analysis of slightly larger systems than otherwise possible. Nevertheless, the size of the matrices still grows exponentially and therefore no fundamentally new window of exploration is opened.

We focus on fermionic models, that is where a Fock state wave function can be written as a string of binary digits, and we consider translational, reflection, and parity invariance. Define the operators  $\mathcal{T}$ ,  $\mathcal{R}$ , and  $\mathcal{P}$  for these operations respectively. Each of these symmetry operators  $\mathcal{S} \in \{\mathcal{T}, \mathcal{R}, \mathcal{P}\}$  commute with the Hamiltonian,  $[H, \mathcal{S}] = 0$ , and each has an order  $n$  for which  $\mathcal{S}^n = 1$ . Thus,  $\mathcal{S}$  must have  $n$  eigenvalues  $\lambda_k = e^{2\pi i k/n}$ . The symmetry operators and their eigenvalues are summarized in table 3.1. Each of these operators will reduce the Hilbert space into their respective subspaces, thus reducing the dimensionality accordingly. However, they do not commute with each other, e.g.  $[\mathcal{T}, \mathcal{R}] \neq 0$ , so it may not be possible to reduce the complexity with all operators simultaneously. However,  $[\mathcal{P}, \mathcal{T}] = 0$ , so we

**Table 3.1:** The symmetry operators of a generic spin chain and their eigenvalues and -states.  $|\chi\rangle$  is an eigenstate of the Hamiltonian.

Name	Symbol	Order	Eigenvalues	Eigenstates
Translation	$\mathcal{T}$	$N$	$\eta_k = \exp(2\pi i k/N)$	$\sum_{n=0}^{N-1} e^{2\pi i k n/N} \mathcal{T}^n  \chi\rangle$
Reflection	$\mathcal{R}$	2	$r = \pm 1$	$(\mathbf{1} \pm \mathcal{R}) \chi\rangle$
Parity change	$\mathcal{P}$	2	$p = \pm 1$	$(\mathbf{1} \pm \mathcal{P}) \chi\rangle$

exploit these two symmetries simultaneously to block-diagonalize the Hamiltonian. The size of the matrix for a given partition of the Hilbert space with quantum numbers  $(k, p)$  is denoted  $N_{(k,p)}$ .

If we look at the translation operator, this will provide the greatest reduction of the Hilbert space since it has the largest number of different eigenvalues, while the parity operator will split the Hilbert space in two. Given a state  $|\chi\rangle$ , not all values of  $k$  are allowed though, e.g. look at the state  $|\chi\rangle = |0101\rangle$ ;

$$\begin{aligned} & (\mathbf{1} + e^{2\pi ik/4}\mathcal{T} + e^{4\pi ik/4}\mathcal{T}^2 + e^{6\pi ik/4}\mathcal{T}^3) |\chi\rangle \\ &= (1 + e^{\pi ik}) |0101\rangle + (e^{\pi ik/2} + e^{3\pi ik/2}) |1010\rangle \\ &= (1 + e^{\pi ik}) (|0101\rangle + e^{\pi ik/2}|1010\rangle). \end{aligned}$$

The latter expression is zero unless  $k = 0$  or  $k = 2$ , and hence  $k = 1$  and  $k = 3$  do not correspond to eigenvalues of the operator. More generally, if  $\mathcal{T}^s|\chi\rangle = |\chi\rangle$  for an  $s \leq N$  and some state  $|\chi\rangle$ , then  $N/s$  must be an integer, and  $k$  must be a multiple of this integer to be a valid quantum number. The two extreme cases are if  $s = N$ , e.g.  $|0001\rangle$ , when all  $k = 0, \dots, N - 1$  are good quantum numbers and if  $s = 1$ , e.g.  $|0000\rangle$ , when only  $k = 0$  is a good quantum number. Hence, for a given state  $|\chi_i\rangle$ , there exists  $s_\chi$  valid  $k$ -quantum numbers, where  $s_\chi$  is the number of unique states that  $|\chi\rangle$  can be transformed into through the translation operator. We have observed that the ground state always is in the  $k = 0$  segment of the Hilbert space, at least assuming there is no spontaneous violation of translation invariance.

To exemplify, the  $N = 4$  Hamiltonian is a  $16 \times 16$  matrix. This can be reduced according to Table 3.2 into groups with a defined parity and wave number. As we see, the matrix is reduced into one  $4 \times 4$  and smaller matrices. In any one of these eight groups, each generating state  $|\chi\rangle$  defines a translationally invariant state,

$$|\psi_\chi^{(k,p)}\rangle = \frac{1}{\sqrt{s_\chi}} \sum_{n=0}^{s_\chi-1} e^{2\pi i kn/N} \mathcal{T}^n |\chi\rangle.$$

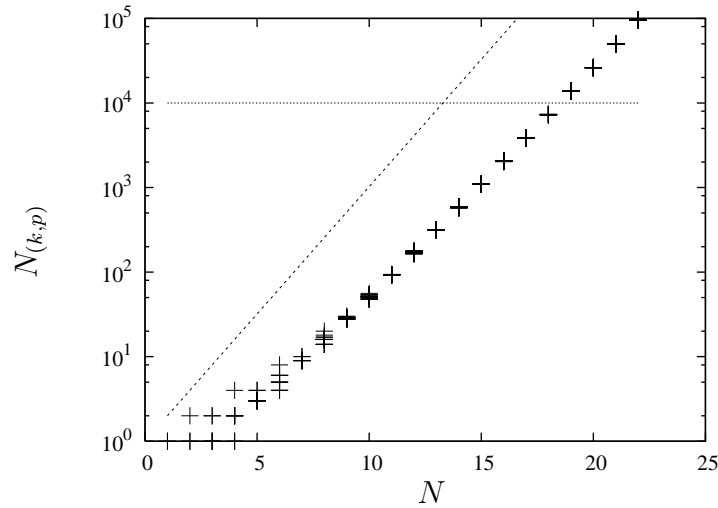
Now each element of the new  $N_{(k,p)} \times N_{(k,p)}$  Hamiltonian matrix  $h$  is

$$h_{\chi\chi'}^{(k)} = \langle \psi_\chi^{(k)} | H | \psi_{\chi'}^{(k)} \rangle = \sum_{n=0}^{s_\chi-1} \sum_{m=0}^{s_{\chi'}-1} \langle \chi | \mathcal{T}^n H \mathcal{T}^m | \chi' \rangle e^{2\pi i k(n-m)/N}$$

for two generating states  $|\chi\rangle$  and  $|\chi'\rangle$ . Hence the computational complexity is reduced somewhat. Figure 3.1 shows how large the submatrices are for different system sizes. The figure shows that with a computational threshold that restrict matrix diagonalization upwards to  $N = 10^4$ , the size of the system that can be considered is increased from  $N = 13$  to  $N = 18$ , which can be a crucial improvement in certain context, such as the criticality detection discussed in Section 5.4.5. Also, one may go beyond this threshold when looking at individual points in the parameter space, but if scanning through a large portion of the space one would usually apply smaller system sizes to avoid excessive time consumption.

**Table 3.2:** The groups when using translational and parity symmetries in a fermionic spin chain of size  $N = 4$ .

Quantum numbers	$ \chi\rangle$	$s_\chi$	$N_{(k,p)}$
$k = 0, p = 1$	$ 0000\rangle$	1	4
	$ 0011\rangle$	4	
	$ 0101\rangle$	2	
	$ 1111\rangle$	1	
$k = 1, p = 1$	$ 0011\rangle$	4	1
$k = 2, p = 1$	$ 0011\rangle$	4	2
	$ 0101\rangle$	2	
$k = 3, p = 1$	$ 0011\rangle$	4	1
$k = 0, p = -1$	$ 0001\rangle$	4	2
	$ 0111\rangle$	4	
$k = 1, p = -1$	$ 0001\rangle$	4	2
	$ 0111\rangle$	4	
$k = 2, p = -1$	$ 0001\rangle$	4	2
	$ 0111\rangle$	4	
$k = 3, p = -1$	$ 0001\rangle$	4	2
	$ 0111\rangle$	4	

**Figure 3.1:** The reduction in complexity when utilizing symmetry as measured by the size of the matrices needed to diagonalize. The dashed line is  $2^N$ , which is the size of the matrix if no symmetries are used, while the points are the size of the matrices in each  $(k, p)$  segment of the Hilbert space. For illustration the horizontal line  $N_{(k,p)} = 10^4$  is shown as a threshold for how large matrices we can diagonalize, and the improvement when using symmetries is from  $N = 13$  to  $N = 18$ .

## 3.2 Renormalization techniques

Renormalization in classical condensed matter systems was conceived by Leo P. Kadanoff in 1966 [Kad66], while Wilson [Wil75] refined the method and applied it to critical phenomena such as the Kondo effect. The basic realization is that at critical points, the system becomes scale invariant, that is the thermodynamic properties can be derived from what happens on large length scales. Hence, one can construct a mapping of a group of lattice sites onto a “supersite” whose properties are derived from the smaller group. This can now be iterated to successively larger blocks until the thermodynamic properties can be extracted. This is known as the renormalization group (RG), and it creates a renormalization flow in the parameter space. The technique has proved highly successful in classical lattice models, and has become a part of the standard theory of critical phenomena.

However, the RG method fails spectacularly for some very simple models, such as the one dimensional particle in a box problem. The very problem that is often used as the first example in quantum mechanics textbooks could not be solved by this approach. White and Noack [WN92] identified the crucial point, that the ground state wave function which is a sine wave, cannot be composed of the ground states of smaller partitions which are also sine waves but with different end points. White thus proposed a new renormalization group, the density matrix renormalization group (DMRG), which picks out the relevant wave functions to keep in further iterations very effectively [Whi92]. In brief, the technique amounts to dividing the full system into a “system”, an “environment”, and two single sites between them that work as a connection. Now, the ground state of this so-called superblock is found as a first approximation. The procedure is then iterated by shrinking the system until it consists of a single site and then growing the system until it reaches a threshold size, and so on until the desired accuracy is reached [Sch05]. This has proven successful for a number of models, such as the above particle in a box and more real problems such as the Heisenberg model, and has established itself as the predominant method for solving low-level excitations in one dimensional systems.

However, the DMRG fails to reproduce the algebraic decay of the correlation functions at the critical point, which is a crucial requirement for any such technique. It has been conjectured that this is because, while the DMRG technique takes some of the entanglement into consideration, it does not preserve maximal entanglement under renormalization [ON02b]. At a critical point it seems that the entanglement constitutes a major part of the wave function, such that an RG technique to estimate e.g. the ground state wave function here must take entanglement into account.

There have been a number of suggestions surfacing in the latest years, such as the entanglement renormalization [Vid05], which tries to devise a new renormalization scheme based on projecting out the most entangled states. Another approach based on so-called projected entangled pair states (PEPS) [VC04, VWPGC06] enables efficient computation in two or more dimensions.

Some issues concerning entanglement properties of the ground state in the Ising chain are addressed in [Skr06a]. In particular, we see that even though the entanglement is a highly important attribute of the wave function, and especially so at the critical point in the Ising chain, there are very few terms in the Schmidt decomposition that needs to be taken into account to construct the wave function. However, it is not yet clear how one should proceed to identify these terms *a priori*, that is when the wave function is not previously known as is the case with the Ising chain. Nevertheless, it is enough to know the first four terms in the Schmidt decomposition of a spin chain with  $N = 100$  spins to determine the entropy with an accuracy of  $10^{-4}$ .

---

## 4 Continuous Variables

---

Usually quantum information theory is occupied with two-level quantum systems, both due to its simplicity and its obvious connection to classical information theory. In particular, the analogy that classical bits are substituted with quantum bits in a quantum computer is appealing, but quantum information in systems with more than two levels, or even a continuous spectrum, is also considered. Such systems are experimentally important since they are easy to generate and manipulate, and quantum information based on quantum optics is arguably where most effort is done implementing feasible quantum systems. Particularly, optical realizations are important in quantum communication. In this chapter we will study continuous variable (CV) systems, that is where each entity can have an infinite number of eigenvalues rather than the two-level system of a qubit. The infinite number of eigenvalues corresponds to the fact that any given mode of the system may contain an arbitrary number of particles, denoted  $|n\rangle$  with  $n = 0, 1, 2, \dots$ . The canonical example of a CV system is the textbook harmonic oscillator, which has an infinite set of discrete energy eigenvalues  $E_n = \omega(n + 1/2)$ . The density matrix of such a system is, in contrast to the fermionic case, infinite dimensional. This means a very different approach to computing physical properties, and also that the entanglement of a state is not bounded upwards as opposed to the fermionic case.

Generally, a CV system of  $N$  particles, or modes, consists of  $N$  conjugate pairs  $x_k$  and  $p_k$  that satisfy the canonical commutation relations

$$[x_k, p_l] = i\delta_{kl}. \quad (4.1)$$

It is customary to define the annihilation and creation operators

$$a_n = \frac{1}{\sqrt{2}}(x_n + ip_n) \quad a_n^\dagger = \frac{1}{\sqrt{2}}(x_n - ip_n), \quad (4.2)$$

which satisfy the commutation relations  $[a_n, a_m^\dagger] = \delta_{nm}$ .

The conventional way to define the density operator is in terms of  $\mathbf{x}$  and  $\mathbf{p}$ ,  $\rho(\mathbf{x}, \mathbf{p})$ . We can also explicitly write down the density matrix in the position basis, in which it is a continuous matrix  $\rho(\mathbf{x}, \mathbf{x}') = \sum_n \psi_n^*(\mathbf{x}) \rho(\mathbf{x}', \mathbf{p}') \psi_n(\mathbf{x}')$  in a choice of basis with basis vectors  $\{\psi_n(\mathbf{x})\}$ . This normalizes as  $\int \rho(\mathbf{x}, \mathbf{x}) d^{2N} \mathbf{x} = 1$  and the expectation value of an operator  $\mathcal{O}(\mathbf{x}, \mathbf{p})$  is

$$\langle \mathcal{O}(\mathbf{x}, \mathbf{p}) \rangle = \text{Tr } \mathcal{O}(\mathbf{x}, \mathbf{p}) \rho(\mathbf{x}, \mathbf{x}'). \quad (4.3)$$

However, it is not always convenient to write the states in the explicit position representation, and we will review the equivalent Weyl representation of the states below.

Separability criteria for CV systems have been proven [GKLC01], and we will here recite some of the important aspects of the continuous variable systems in terms of Gaussian states and refer to the proofs in the literature.

## 4.1 Weyl algebra

Continuous variable states as defined by the  $x_k$  and  $p_k$  operators can be conveniently formulated in terms of the Weyl algebra. To this end, we define the  $2N$  operators  $r_k$  as

$$\mathbf{r} = [x_1, p_1, x_2, p_2, \dots, x_N, p_N]^T. \quad (4.4)$$

These operators' commutation relations can be written as

$$[r_k, r_l] = iJ_{kl} \quad (4.5)$$

where  $J$  is the  $2N \times 2N$  matrix

$$J = \bigoplus_{k=1}^N \begin{bmatrix} 0 & 1 \\ -1 & 0 \end{bmatrix}. \quad (4.6)$$

This matrix is the defining matrix of the symplectic group  $\text{Sp}(2N)$ , which is the group under multiplication of all  $2N \times 2N$  matrices  $M$  that satisfy

$$M^T J M = J. \quad (4.7)$$

Now we may define the Weyl operators which are defined on  $\xi \in \mathbb{R}^{2N}$  as

$$\mathcal{W}(\xi) = \exp \left( -i \sum_k \xi_k r_k \right). \quad (4.8)$$

Finally, defining the form  $\sigma(\xi, \zeta) = \sum_{ij} \xi_i J_{ij} \zeta_j$ , the Weyl relations are

$$\mathcal{W}(\xi) \mathcal{W}(\zeta) = e^{-i\sigma(\xi, \zeta)} \mathcal{W}(\zeta) \mathcal{W}(\xi). \quad (4.9)$$



Given a quantum state  $\rho$ , the characteristic function  $\chi(\xi)$  of the state is simply the expectation value of the Weyl operators,

$$\chi(\xi) = \text{Tr } \rho \mathcal{W}(\xi). \quad (4.10)$$

Inversely, the density matrix can be written in terms of the characteristic function and the Weyl operators,

$$\rho = \frac{1}{(2\pi)^N} \int \chi(\xi) \mathcal{W}(-\xi) \, d^{2N} \xi. \quad (4.11)$$

All expectation values of polynomials of the canonical operators  $r_k$  can be expressed in terms of differentiations of the characteristic functions. Indeed, the two first momenta are

$$\langle r_k \rangle = i \frac{\partial}{\partial t} \chi(t \hat{e}_k) \Big|_{t=0} \quad (4.12a)$$

$$\langle r_k r_l \rangle = - \frac{\partial^2}{\partial t_1 \partial t_2} e^{-\frac{i}{2} t_1 t_2 J_{kl}} \chi(t_1 \hat{e}_k + t_2 \hat{e}_l) \Big|_{t_1=t_2=0}, \quad (4.12b)$$

where  $\hat{e}_k$  is the unit vector of element  $k$ .

According to the above, the formulation of the theory with Weyl operators is equivalent to the formulation with canonical operators. Hence, which one is applied is a matter of taste and computational convenience. A general state in the form of a density matrix is completely determined by all  $n$ th order momenta. However, we will focus on the important class of Gaussian states. These are experimentally important due to the simplicity involved in creating and manipulating them. Also, they are simple and elegant to compute analytically but nevertheless involves a rich structure. Further, for the Gaussian states only the first and second order momenta are necessary to completely determine the state. This is of course a convenient situation where both experimental and theoretical simplicity meets and Gaussian states are therefore by far the most studied continuous variable states in both camps.

## 4.2 Gaussian states

A state  $\rho$  is called Gaussian if its characteristic function is a Gaussian,

$$\chi(\xi) = \exp \left[ -\frac{1}{4} \sum_{ij} \xi_i \Gamma_{ij} \xi_j + i \sum_i \delta_i \xi_i \right]. \quad (4.13)$$

The  $2N \times 2N$  matrix  $\Gamma$  must be positive and symmetric to give rise to finite expectation values.  $\Gamma$  is known as the correlation matrix and  $\delta \in \mathbb{R}^{2N}$  as the displacement vector. Equivalently, and according to the convention used in [Skr05a], a Gaussian state can be

written in the position basis as

$$\begin{aligned} \rho(\mathbf{q}, \mathbf{q}') &= \sqrt{\frac{\det(A' - C')}{\pi^D}} \exp \left[ -d'_i (A'_{ij} - C'_{ij})^{-1} d'_j \right] \\ &\quad \times \exp \left[ -\frac{1}{2} (q_i A_{ij} q_j + q'_i A^*_{ij} q'_j) + q_i C_{ij} q'_j + d_i q_i + d_i^* q'_i \right]. \end{aligned} \quad (4.14)$$

Here  $A' = \text{Re } A$ ,  $C' = \text{Re } C$ , and  $d' = \text{Re } d$  with  $A$  and  $C$   $N \times N$  matrices and  $d$  an  $N$  dimensional vector. The equivalence of the two formulations is evident when we compute the first and second order momenta from Eqs. (4.12) and from direct calculation on the density matrix. To simplify the equations we consider the variational matrices

$$Q_{kl} = \langle q_k q_l \rangle - \langle q_k \rangle \langle q_l \rangle \quad (4.15a)$$

$$P_{kl} = \langle p_k p_l \rangle - \langle p_k \rangle \langle p_l \rangle \quad (4.15b)$$

$$S_{kl} = \frac{1}{2} \langle q_k p_l + p_l q_k \rangle - \langle q_k \rangle \langle p_l \rangle. \quad (4.15c)$$

Computing these for both formulations, we find

$$Q_{kl} = \Gamma_{2k-1, 2l-1} = \frac{1}{2} \{ (\text{Re } A - \text{Re } C)^{-1} \}_{kl} \quad (4.16a)$$

$$P_{kl} = \Gamma_{2k, 2l} = A_{kl} - (A_{ki} - C_{ki}) Q_{ij} (A_{jl} - C_{jl})^T \quad (4.16b)$$

$$S_{kl} = \frac{1}{2} \Gamma_{2k-1, 2l} = -Q_{ki} (\text{Im } A_{il} + \text{Im } C_{il}) \quad (4.16c)$$

$$\langle q_k \rangle = \xi_{2k-1} = 2Q_{ki} \text{Re } d_i \quad (4.16d)$$

$$\langle p_k \rangle = \xi_{2k} = -2(\text{Im } A_{ki} - \text{Im } C_{ki}) Q_{ij} \text{Re } d_j + \text{Im } d_k. \quad (4.16e)$$

This shows the mapping between the two formulations, and though they are equivalent, the mapping is complicated. However, the position representation gives a more physical view that counters the mathematical convenience of the Weyl representation.

As shown in [Skr05a], using the position representation one can perform a rotation, scaling and another rotation of the coordinate system to separate the density matrix into single particle density matrices for  $N$  virtual particles. Having found this transformation, it is easy to find the eigenvalues of the single particle density matrices and thus the eigenvalues of the full density matrix. Also, we show that the massless Klein-Gordon field possesses conformal symmetries (see Section 5.2), and that this can be identified by the entanglement signatures in the model.

It is easy to realize that a state with  $C = 0$  is separable with  $\rho(\mathbf{q}, \mathbf{q}') = \rho_1(\mathbf{q})\rho_2(\mathbf{q}')$ , and thus a pure state. Indeed, this is a necessary criterion, and for the Weyl formulation this is equivalent to  $\det \Gamma = 1$ .

### 4.3 The Klein-Gordon field

As our main example of a bosonic field we use the simplest possible, namely the free Klein-Gordon field placed on a  $1 + 1$  dimensional chain with periodic boundary conditions. That is, we use the Lagrangian

$$\mathcal{L} = \sum_n [\dot{\varphi}_n^2 - (\nabla\varphi_n)^2 - \kappa^2\varphi_n^2] \quad (4.17)$$

summed over all lattice points. The Euler-Lagrange equations gives the equations of motion and the dispersion relation

$$\omega_k^2 = \frac{4}{a^2} \sin^2(k/2) + \kappa^2 \quad (4.18)$$

where  $a$  is the lattice constant. To maintain a conformal invariance of the model, one must keep  $Na$  constant when rescaling the theory. Now follow the expectation value matrices for the ground state of the field,

$$Q_{mn} = \frac{1}{2N} \sum_k \frac{1}{\omega_k} e^{ik(m-n)} \quad (4.19)$$

$$P_{mn} = \frac{1}{2N} \sum_k \omega_k e^{ik(m-n)} \quad (4.20)$$

$$S_{mn} = 0. \quad (4.21)$$

The sums over  $k$  are over all wave numbers  $2\pi n/N$  with  $n = \{0, \dots, N - 1\}$ , discretized through the boundary conditions.

In the massless limit, the field is expected to be conformal, and thus follows the conformal signature derived by Holzhey, Larsen, and Wilczek [HLW94, Skr05a] (see Section 5.2). Massless here means roughly  $\kappa \leq 0.1$ . The true massless system  $\kappa = 0$  is not accessible as  $Q$  diverges due to the  $k = 0$  term. A massive theory in the limit  $\kappa \rightarrow \infty$  carries no entanglement.

One can also impose anti-periodic boundary conditions on the field, thereby explicitly violating the translational invariance in the target space, and hence the conformal symmetry. The entanglement diverges as  $N \rightarrow \infty$ , like in the periodic case. However, in the limit  $\kappa \rightarrow 0$  the periodic wave function leads to diverging entanglement, while the anti-periodic one does not. This is an example of entanglement divergence even though we do not have conformal invariance. Usually, in non-critical systems, the entanglement saturates at some point.

## 4.4 Two-mode entanglement

The reduced density matrix of two sites in the lattice is generally a mixed state, and generally the entanglement in this state is ill-defined. However, for Gaussian CV states, it is known how to find the entanglement of formation for this state [WGK<sup>+</sup>04]. That is, the so-called Gaussian entanglement of formation  $E_G$  of a state  $\rho_\Gamma$  with correlation matrix  $\Gamma$  is

$$E_G(\rho_\Gamma) = \inf_{\Gamma_p} \{S(\rho_{\Gamma_p}) | \Gamma_p \leq \Gamma\} \quad (4.22)$$

where  $\Gamma_p$  are correlation matrices of all pure states and  $S(\rho_{\Gamma_p})$  is the von Neumann entropy of the state. For the case of Gaussian states this is determined by the correlation matrix' symplectic eigenvalues. Given a symmetric, positive matrix  $\Gamma$ , one can find a symplectic matrix  $M \in \text{Sp}(2N)$  and a diagonal matrix  $D \in \mathbb{R}^{N \times N}$  such that

$$M\Gamma M^T = D \oplus D. \quad (4.23)$$

This is known as the symplectic diagonalization of  $\Gamma$ , and it is unique up to permutations. The elements of  $D = \text{diag}(d_1, \dots, d_N)$  are known as the symplectic eigenvalues of  $\Gamma$ . Now, the von Neumann entropy of the pure state  $\Gamma_p$  is [WGK<sup>+</sup>04]

$$S(\rho_{\Gamma_p}) = \sum_k \zeta(\alpha_k) \quad (4.24)$$

where

$$\begin{aligned} \zeta(x) &= \cosh^2(x) \log_2(\cosh^2 x) - \sinh^2(x) \log_2(\sinh^2 x) \\ d_k &= \cosh \alpha_k, \quad \alpha_k \geq 0. \end{aligned} \quad (4.25)$$

Given a 1+1D chain of bosonic systems, one can write the correlation matrix for two sites, known as the two-mode correlation matrix, as

$$\Gamma = \begin{bmatrix} q_0 & 0 & q_1 & 0 \\ 0 & p_0 & 0 & p_1 \\ q_1 & 0 & q_0 & 0 \\ 0 & p_1 & 0 & p_0 \end{bmatrix} = \Gamma_q \otimes \begin{bmatrix} 1 & 0 \\ 0 & 0 \end{bmatrix} + \Gamma_p \otimes \begin{bmatrix} 0 & 0 \\ 0 & 1 \end{bmatrix} \quad (4.26)$$

where

$$\Gamma_q = \begin{bmatrix} q_0 & q_1 \\ q_1 & q_0 \end{bmatrix} \quad \text{and} \quad \Gamma_p = \begin{bmatrix} p_0 & p_1 \\ p_1 & p_0 \end{bmatrix}.$$

Here  $q_0 = Q_{00}$ ,  $q_1 = Q_{0n}$ ,  $p_0 = P_{00}$ , and  $p_1 = P_{0n}$  with  $n$  the distance between the two sites under consideration. Generally, any two-mode correlation matrix can under local unitary transformations be written in the so-called standard form

$$\tilde{\Gamma} = \begin{bmatrix} n_a & 0 & k_q & 0 \\ 0 & n_a & 0 & k_p \\ k_q & 0 & n_b & 0 \\ 0 & k_p & 0 & n_b \end{bmatrix} \quad (4.27)$$

with  $k_q \geq |k_p|$ . For the special case that  $n_a = n_b = n$ , the state is known as a symmetric state [GWK<sup>+</sup>03] and a necessary condition for this to be a correlation matrix is that  $n^2 - k_q^2 \geq 1/4$ . Also, the state is entangled if and only if  $(n - k_q)(n + k_p) < 1$  [GKLC01]. Symmetric states arise for example as two light beams from a parametric down converter is sent through optical fibres or when a squeezed state is sent through two identical lossy fibres. The entanglement of the symmetric Gaussian state is particularly simple,

$$E_G(\rho_\Gamma) = \zeta(p), \quad p = \frac{1}{2} \ln [(n - k_q)(n + k_p)] \quad (4.28)$$

with  $\zeta(x)$  defined in (4.25). In terms of the correlation matrix this can be written as a symmetric state through the symplectic transformation

$$S = \text{diag}(\sqrt{\eta}, 1/\sqrt{\eta}, \sqrt{\eta}, 1/\sqrt{\eta})$$

where  $\eta$  is the squeezing factor  $\eta = \sqrt{p_0/q_0}$ . This is a local, unitary Gaussian operation. Hence

$$n = \sqrt{q_0 p_0} \quad k_q = q_1 \sqrt{\frac{p_0}{q_0}} \quad k_p = p_1 \sqrt{\frac{q_0}{p_0}}, \quad (4.29)$$

and the entanglement follows from this.

Some results for the Klein-Gordon field is shown in Fig. 4.1. We see that the entanglement in the massless field vanishes quickly with distance, indeed for large systems the entanglement extends only to the nearest neighbor. For small systems it may extend to the third neighbor, due to the periodic boundary conditions. Also, all entanglement vanish for a massive system of  $\kappa \gtrsim 1$ , as is the case for the entanglement entropy [Skr05a]. However, there is no divergent entanglement for the two-mode case as opposed to the entanglement entropy, but the entropy saturates for  $N \rightarrow \infty$ ,  $\kappa \rightarrow 0$  at  $E_G \approx 0.48$ .

## 4.5 State evolution

The massless Klein-Gordon field, or the bosonic vacuum investigated in [Skr05a] gives directly rise to a conformal symmetry and the properties that can be deduced from that. However, the time evolution of a state in vacuum is trivial, and to provoke a non-trivial time evolution of the system, we introduce an impurity and consider the toy model with Lagrangian density

$$\mathcal{L}_n = \frac{1}{2} [\dot{\varphi}_n^2 - (\nabla \varphi_n)^2 - \kappa^2 \varphi_n^2] + \varepsilon \delta_{nl}. \quad (4.30)$$

This is the usual Klein-Gordon field bracketed and an impurity of strength  $\varepsilon$  at a site  $l$  to provoke a non-trivial time evolution of the state. The system is still linear, and the discussion of this system is an example of how linear systems can still provide interesting behaviour. We assume the initial condition that the initial state is that of the unperturbed case  $\varepsilon = 0$ .

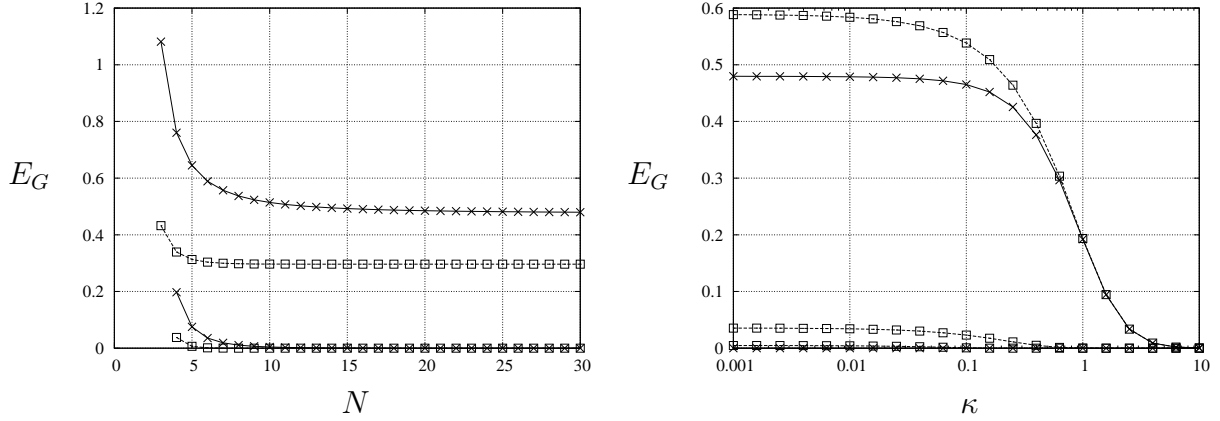


**Figure 4.1:** The two-mode Gaussian entanglement between two sites in the 1D Klein-Gordon field with periodic boundary conditions.

*Left:*  $E_G$  for the nearest neighbor and next-nearest neighbor as function of total system size  $N$ . The data are for a massless ( $\kappa = 10^{-3}$ ,  $\times$ ) and a massive ( $\kappa = 10^{-0.2}$ ,  $\square$ ) system. The next-neighbor entanglement vanishes for large systems, while the 3rd neighbor entanglement is non-zero only for  $N = 6$ .

*Right:*  $E_G$  for the three nearest neighbor pairs as function of  $\kappa$  for a large ( $N = 30$ ,  $\times$ ) and a small ( $N = 6$ ,  $\square$ ) system.

We apply periodic boundary conditions, and Fourier expanding the field in the Heisenberg picture gives

$$\varphi_n(t) = \sum_k \frac{1}{\sqrt{2N\omega_k}} \left[ a_k(t)e^{ikn} + a_k^\dagger(t)e^{-ikn} \right] \quad (4.31)$$

with the initial condition  $a_k(0) = a_k$ . The time evolution of the operators  $a$  and  $a^\dagger$  can now be computed by the Euler-Lagrange equations to be

$$a_k(t) = a_k e^{-i\omega_k t} + \frac{h_k}{\omega_k^2} (1 - e^{-i\omega_k t}), \quad (4.32)$$

where

$$\omega_k^2 = \frac{4}{a^2} \sin^2(k/2) + \kappa^2 \quad \text{and} \quad h_k = \sqrt{\frac{\omega_k}{2N}} \varepsilon e^{-ikl}.$$

Now, we consider the vacuum state  $|\Omega\rangle$ , that is the ground state of the unperturbed system where  $a_k|\Omega\rangle = 0$ . Then the correlation matrix is unchanged, but the expectation values of the field become

$$\langle \varphi_n(t) \rangle = \frac{\varepsilon}{N} \sum_k \frac{1}{\omega_k^2} [\cos k(n-l) - \cos(\omega_k t - k(n-l))], \quad (4.33)$$

and, if we consider the site of the impurity,  $n = l$  we find the equation of motion

$$\langle \varphi_n(t) \rangle = \frac{\varepsilon}{N} \sum_k \frac{1}{\omega_k^2} (1 - \cos \omega_k t). \quad (4.34)$$

When  $N \rightarrow \infty$  we can write the constant term as

$$\frac{\varepsilon}{N} \sum_k \frac{1}{\omega_k^2} = \frac{\varepsilon}{\pi} \int_0^\pi \frac{1}{\omega_k^2} = \frac{\pi a}{\kappa \sqrt{4 + \kappa^2 a^2}}. \quad (4.35)$$

Figures 4.2 show the time evolution of the field expectation value  $\langle \varphi_n(t) \rangle$  and its derivative, the expectation value of the conjugate field  $\langle \pi_n(t) \rangle = \langle \dot{\varphi}_n(t) \rangle$ . The field has a roughly cosine shape, governed by the main contributing  $k = 0$  term (“the zero-mode”) of the sum 4.33. Hence the period is  $2\pi\kappa^{-1}$ . Also, given that we consider the impurity term, a new perturbation hits this site every time a perturbation has propagated through the system to the site. Thus, with units where the perturbation speed in the system equals the lattice constant per time unit, there will be a new perturbation every  $N$  time units. If we consider another site  $\delta$  sites away from the perturbation site, the perturbation will hit every  $\delta + Nn$  and  $N - \delta + Nn$  time units with integer  $n$ . In the following we consider the impurity points and units where the perturbation speed is one lattice point per time unit and an invariant lattice constant  $a = 1$ . Now, we have two different regimes dependent on  $\kappa N \leq 2\pi$ . For large systems where  $\kappa N > 2\pi$ , the main contribution is the oscillations of the point itself.

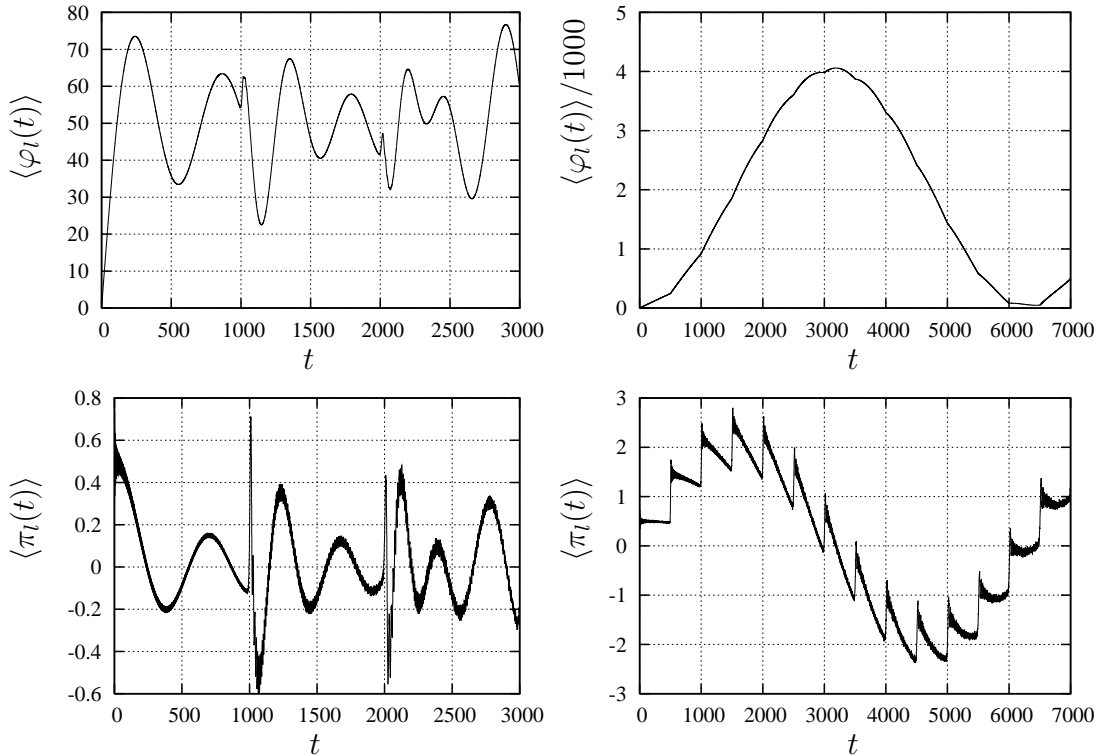


**Figure 4.2:** The field expectation values  $\langle \varphi_l(t) \rangle$  and  $\langle \pi_l(t) \rangle$  at the perturbation site  $l$  with time. To the left  $\kappa = 10^{-2}$  and  $N = 1000$  ( $\kappa N = 10 > 2\pi$ ), and to the right  $\kappa = 10^{-3}$  and  $N = 500$  ( $\kappa N = 0.5 < 2\pi$ ). Note that a perturbation hits every  $N$  time units and that the predominant oscillations have period  $2\pi\kappa^{-1}$ .

The field tends to relax its oscillation over time until a perturbation hits which excites the field again, followed by another relaxation period. For small systems with  $\kappa N < 2\pi$  the relaxation never occurs since the perturbation hits the point too quickly, and thus the perturbations are the main contribution to the time evolution. Figures 4.2 illustrate these two regimes. In both cases the leading oscillatory term is with frequency  $2\pi\kappa^{-1}$ , even though the main oscillations have different origins. Also, the expectation value  $\langle\pi_l(t)\rangle$  has small oscillations of frequency  $2\pi$ , which in the figure appears as a smearing of the graph.



---

## 5 Quantum Critical Systems

---

Classical phase transitions occur under the change of temperature where at some critical temperature  $T_c$  the system has an abrupt thermodynamical change, the hallmark example being the liquid-solid transition in e.g. water. Quantum phase transitions [Sac99] occur at zero temperature, and thus quantum effects can automatically be assumed to be profound. Indeed, the thermal fluctuations that take a classical state across a phase transition are non-existent, and the only fluctuations present are the quantum fluctuations determined by Heisenberg's uncertainty principle.

The general setup is to consider a quantum system under the change of some external parameter  $\gamma$ , which causes a transition at some critical value  $\gamma_c$ , where a previously excited state now becomes the ground state. This crossover is called the quantum critical point. At this critical point there are, just as in classical phase transitions, scaling laws. For example the energy gap  $\Delta$ , which necessarily is zero at the transition itself, will scale as

$$\Delta \sim J|\gamma - \gamma_c|^{z\nu}$$

where  $z\nu$  is known as the critical exponent of the phase transition and  $J$  is some energy scale. Moreover, the correlation length  $\xi$  will diverge (in an infinite system) at the critical point, and scale according to  $\xi \sim L|\gamma - \gamma_c|^{-\nu}$ . This also means that we have a scaling law between the correlation length and the energy gap,

$$\Delta \sim \xi^{-z}.$$

Since the correlation length diverges – or extends to the entire system in the case of a finite system size – the system is scale invariant at the critical point, and the properties of the system becomes independent of the scale on which we view the system.

Any classical phase transition invariably has temperature fluctuations which drive the phase transition. However, as the quantum phase transitions occur at  $T = 0$ , there can be no classical fluctuations in these models. Nevertheless there are always quantum fluctuations

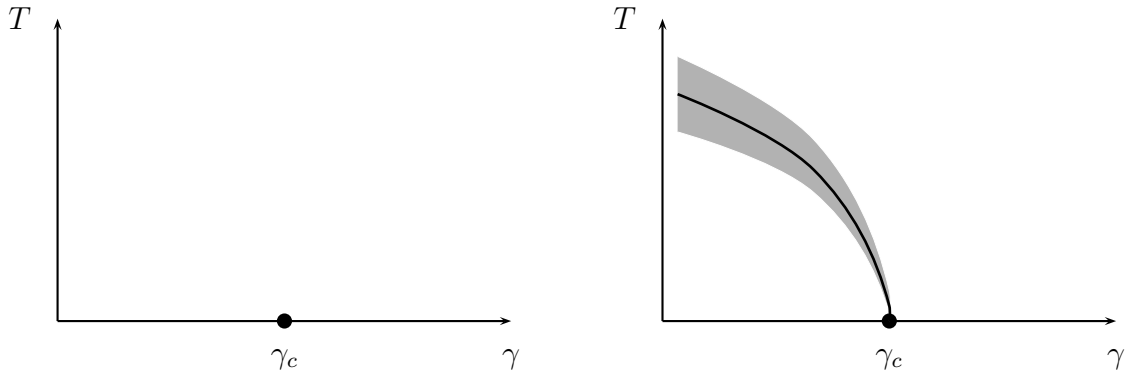


**Figure 5.1:** Two scenarios for a quantum phase transition in which a parameter  $\gamma$  is taken across the critical value  $\gamma_c$ . To the left there is no classical phase transition close to the quantum transition, while to the right there is a classical phase transition across the line, and in the shaded region the theory of classical phase transitions can be applied. [Sac99]

due to Heisenberg's uncertainty principle, and these fluctuations have to drive the quantum transition, in the sense that they are necessary to explore the low-lying excitations of the system. Moreover, the classical correlations present in the classical models can be partially replaced by the quantum correlations which present themselves as entanglement.

The quantum phase transition may or may not have a classical counterpart in the  $T > 0$  regime, see Fig. 5.1, in which case there will be a region where there are competing classical and quantum fluctuations across the boundary. However, there are also cases where the thermodynamic variables are analytical close to the  $T = 0$  line, and thus no classical phase transition takes place.

In the study of quantum statistical mechanics, we use the density operator, which at finite temperatures take the form

$$\rho = e^{-\beta H},$$

where  $\beta$  is the inverse temperature and  $H$  the Hamiltonian. However, in the zero-temperature limit  $\beta \rightarrow \infty$  only the ground state will contribute to this expression, and assuming the Hamiltonian is diagonal in some basis  $H = \sum_n E_n |n\rangle\langle n|$  with lowest energy level  $E_0 = 0$ , the density operator becomes

$$\rho(T = 0) = e^{-\beta \sum_n E_n |n\rangle\langle n|} = e^{-\beta E_0 |0\rangle\langle 0|} = |0\rangle\langle 0|.$$

Hence, when computing properties of a quantum critical system, we need to identify the ground state and hence follows the density matrix and all thermodynamic properties.

A phase transition can, strictly speaking, only occur in the thermodynamic limit of  $\sim 10^{23}$  particles, which is naturally inaccessible when implementing the system on a computer. However, one may see traces of what may become a phase transition at smaller systems, even with as little as  $\sim 10$  particles [SO05]. However, it is important to emphasize that no

actual phase transition can occur in this system, and that when we speak about parameters where we get a phase transition, it should be interpreted as parameters where a phase transition occurs in the thermodynamic limit.

## 5.1 Ground state entropy

When the ground state of a quantum system changes macroscopic features across a quantum phase transition, the details of the ground state is vastly more complicated at the phase transition point than at non-critical places in the parameter space. This is indicated by the increase of entanglement at the critical point as measured both by the concurrence [OAFF02] and the entanglement entropy [VLRK02, LRV04]. As the entropy involves tracing out some part of the system, it will have a dependence on the size of the system traced out, as well as the overall system size. However, it should not depend on the small-scale details of the models since these are irrelevant at critical points according to renormalization theory.

Specifically, at the critical point in theories where one has conformal invariance in  $1 + 1$  dimension, the entropy diverges logarithmically with system size, as opposed to off-critical points where the entropy saturates [LRV04]. However, close to the critical point, the system size where the entropy saturates is very large, and thus this is not a very efficient indicator of whether or not a system is critical due to the computational resources required.

## 5.2 Consequences of conformal symmetry

Since Polyakov [Pol70] it has been known that local scale invariance implies conformal invariance and that this fact can be used to investigate criticality in statistical mechanical systems. Belavin, Poyakov and Zamolodchikov [BPZ84] showed how the rich structure of two-dimensional conformal theories can be used to extract information on the critical properties of a quantum field theory.

A quantum field theory becomes conformal if it fulfills the following requirements [FMS97, Gin89];

- Translation and rotation invariance
- Local interactions
- Lorentz invariance
- Scale invariance

The last condition is the crucial one, since it is only fulfilled at critical points. Thus we expect conformal symmetry on the critical point, but not elsewhere in the parameter space. The conformal group in two dimensions is infinite as opposed to larger dimensions<sup>1</sup>. That is, any holomorphic transformation is conformal, and to specify a holomorphic transformation means to know all the coefficients of its Laurent series, which are infinitely many. This means that conformal symmetries in two dimensions are easier to analyze and has a richer structure than those in larger dimensionalities, and this is the reason that we will exclusively focus on this case.

We define the real coordinates  $(z^0, z^1)$  on the plane, and introduce complex coordinates,

$$z = z^0 + iz^1 \quad \bar{z} = z^0 - iz^1,$$

with differentiation rules

$$\partial \equiv \partial_z = \frac{1}{2}(\partial_0 - i\partial_1) \quad \bar{\partial} \equiv \partial_{\bar{z}} = \frac{1}{2}(\partial_0 + i\partial_1).$$

Under a holomorphic transformation  $z \mapsto f(z)$ , a line element  $ds^2 = dz d\bar{z}$  transforms as

$$ds^2 \mapsto \left( \frac{\partial f}{\partial z} \right) \left( \frac{\partial \bar{f}}{\partial \bar{z}} \right) ds^2.$$

This transformation law is generalized under the assumption that  $\Phi(z, \bar{z}) dz^h d\bar{z}^{\bar{h}}$  is invariant under the transformation. Here  $\Phi(z, \bar{z})$  is a field and  $h$  and  $\bar{h}$  are real parameters. Then the field transforms as

$$\Phi(z, \bar{z}) \mapsto \left( \frac{\partial f}{\partial z} \right)^h \left( \frac{\partial \bar{f}}{\partial \bar{z}} \right)^{\bar{h}} \Phi(f(z), \bar{f}(\bar{z})). \quad (5.1)$$

This defines a primary field of conformal weight  $(h, \bar{h})$ . Non-primary fields are known as secondary fields.

A key ingredient when computing correlators in conformal symmetry is the operator product expansion (OPE). This is the assumption that the product of two local fields  $\phi_i(x)$  and  $\phi_j(y)$  can be written as a linear combination of local operators,

$$\phi_i(x)\phi_j(y) = \sum_k C_{ij}^k(x-y)\phi_k(y)$$

where the coefficients  $C_{ij}^k$  are c-numbers. Now, one is usually interested in the singular behavior as  $x \rightarrow y$ , and we use  $\sim$  to indicate that regular terms are discarded. For a primary field  $\varphi$  with conformal dimension  $h$ , the OPE of this with the energy momentum tensor is

$$T(z)\varphi(w, \bar{w}) \sim \frac{h}{(z-w)^2}\varphi(w, \bar{w}) + \frac{1}{z-w}\partial_w\varphi(w, \bar{w})$$

---

<sup>1</sup>The one dimensional case is trivial, since any continuous transformation is conformal.

and correspondingly for the anti-holomorphic fields. For the energy-momentum tensor with itself the OPE is

$$T(z)T(w) \sim \frac{c/2}{(z-w)^4} + \frac{2T(w)}{(z-w)^2} + \frac{\partial T(w)}{z-w}. \quad (5.2)$$

The constant  $c$  is called the *central charge* of the specific model in question, or sometimes denoted the conformal anomaly. Apart from this anomaly, the energy-momentum tensor is simply a conformal field of conformal dimension  $h = 2$ . Of course, the relation (5.2) holds also for the anti-holomorphic parts of the theory, thereby defining an independent anti-holomorphic central charge  $\bar{c}$ . When the theory has a Lorentz-invariant and conserved two-point function  $\langle T_{\mu\nu}(z)T_{\alpha\beta}(-z) \rangle$ , one must have  $c = \bar{c}$  [Gin89]. This holds for all relevant quantum statistical systems.

Central in conformal field theories is the study of correlation functions, a subject with obvious connections to critical systems. In particular, the two-point correlation function of two fields  $\phi_1$  and  $\phi_2$  is nonzero if and only if they have the same conformal weights  $h_1 = h_2 = h$  and  $\bar{h}_1 = \bar{h}_2 = \bar{h}$ . Then,

$$\langle \phi_1(z_1, \bar{z}_1)\phi_2(z_2, \bar{z}_2) \rangle = \frac{C_{12}}{(z_1 - z_2)^{2h}(\bar{z}_1 - \bar{z}_2)^{2\bar{h}}}.$$

Notably, the correlation function depends only on the distances  $z_1 - z_2$  and  $\bar{z}_1 - \bar{z}_2$ , a statement that is true also for the three- and four-point correlation functions.

The Laurent expansion of the energy-momentum tensor can be written

$$T(z) = \sum_{n=-\infty}^{\infty} z^{-z-2} L_n \quad \text{and} \quad \bar{T}(\bar{z}) = \sum_{n=-\infty}^{\infty} \bar{z}^{-z-2} \bar{L}_n, \quad (5.3)$$

and the inverse relations are

$$L_n = \oint \frac{dz}{2\pi i} z^{n+1} T(z) \quad \text{and} \quad \bar{L}_n = \oint \frac{d\bar{z}}{2\pi i} \bar{z}^{n+1} \bar{T}(\bar{z}). \quad (5.4)$$

Now, one can compute the commutators of  $L_n$  by performing the integrals and expressing the OPE of the energy-momentum tensor, and the results are

$$\begin{aligned} [L_n, L_m] &= (n-m)L_{n+m} + \frac{c}{12}(n^3 - n)\delta_{n,-m} \\ [\bar{L}_n, \bar{L}_m] &= (n-m)\bar{L}_{n+m} + \frac{\bar{c}}{12}(n^3 - n)\delta_{n,-m} \\ [L_n, \bar{L}_m] &= 0. \end{aligned}$$

Thus we have two independent algebras on  $L_n$  and  $\bar{L}_n$  of infinite dimension. This is known as the Virasoro algebra of the central charge  $c$ . If  $c = 0$ , the algebra defined on  $L_n$  is the classical algebra of the generators for infinitesimal conformal transformations in the plane.

### 5.2.1 The free boson

The free massless boson in two dimensions has an Euclidean action [FMS97]

$$S[\varphi] = \frac{1}{2}g \int d^2x \partial_\mu \varphi \partial^\mu \varphi, \quad (5.5)$$

where  $g$  is a normalization constant. The two-point correlator of this field is

$$\langle \varphi(x) \varphi(y) \rangle = -\frac{1}{4\pi g} \ln(x-y)^2 + \text{const.}$$

When introducing the complex coordinates  $z$  and  $\bar{z}$ , this becomes

$$\langle \varphi(z, \bar{z}) \varphi(w, \bar{w}) \rangle = -\frac{1}{4\pi g} [\ln(z-w) + \ln(\bar{z}-\bar{w})] + \text{const.},$$

or when separating the holomorphic and anti-holomorphic parts through a differentiation, the operator product expansion of the holomorphic field  $\partial\varphi = \partial_z\varphi$  becomes

$$\begin{aligned} \langle \partial_z \varphi(z, \bar{z}) \partial_w \varphi(w, \bar{w}) \rangle &= -\frac{1}{4\pi g} \frac{1}{(z-w)^2} \\ \partial\varphi(z) \partial\varphi(w) &\sim -\frac{1}{4\pi g} \frac{1}{(z-w)^2}. \end{aligned}$$

The bosonic symmetry property of this OPE is immediately obvious. Now, the energy momentum tensor in complex coordinates is

$$T(z) = -2\pi g : \partial\varphi(z) \partial\varphi(z) : \quad (5.6)$$

Here  $: \cdot :$  denotes normal ordering to ensure that vacuum expectation values vanish. Wick's theorem allows us to compute the OPE of the energy-momentum tensor with itself;

$$\begin{aligned} T(z)T(w) &= 4\pi^2 g^2 : \partial\varphi(z) \partial\varphi(z) :: \partial\varphi(w) \partial\varphi(w) : \\ &= 8\pi^2 g^2 : \overbrace{\partial\varphi(z) \partial\varphi(z)} :: \overbrace{\partial\varphi(w) \partial\varphi(w)} : \\ &\quad + 16\pi^2 g^2 : \overbrace{\partial\varphi(z) \partial\varphi(z)} :: \overbrace{\partial\varphi(w) \partial\varphi(w)} : \\ &\sim \frac{1/2}{(z-w)^4} - 4\pi g \frac{\partial\varphi(z) \partial\varphi(w)}{(z-w)^2} \\ &\sim \frac{1/2}{(z-w)^4} + \frac{2T(w)}{(z-w)^2} + \frac{\partial T(w)}{(z-w)}, \end{aligned}$$

the last equation arises by a linear expansion around  $w$ ,  $\partial\varphi(z) = \partial\varphi(w) + (z-w)\partial^2\varphi(w)$ . Thus, the OPE has an anomalous term  $(1/2)/(z-w)^4$  which fixes the central charge of the model at  $c = 1$ , and the energy-momentum tensor is not a primary field.

### 5.2.2 The free fermion

The free fermion in two dimensions is described by the two-component spinor  $\Psi = (\psi, \bar{\psi})$ , and the action is

$$S(\Psi) = g \int d^2x (\bar{\psi} \partial \bar{\psi} + \psi \bar{\partial} \psi). \quad (5.7)$$

The propagator of this field becomes

$$\langle \psi(z, \bar{z}) \psi(w, \bar{w}) \rangle = \frac{1}{2\pi g} \frac{1}{z - w},$$

and thus the OPE follows trivially

$$\psi(z) \psi(w) \sim \frac{1}{2\pi g} \frac{1}{z - w},$$

which of course has fermionic symmetry properties under particle exchange. The energy-momentum tensor is now

$$T(z) = -\pi g : \psi(z) \partial \psi(z) :,$$

and by Wick's theorem we arrive at the OPE for  $T(z)$  with itself;

$$\begin{aligned} T(z)T(w) &= \pi^2 g^2 : \psi(z) \partial \psi(z) :: \psi(w) \partial \psi(w) : \\ &\sim \frac{1/4}{(z-w)^4} + \frac{\pi g}{2} \frac{1}{(z-w)^2} (: \psi(z) \psi(w) : - : \psi(z) \partial \psi(w) : + \partial \psi(z) \psi(w) :) \\ &\quad - \frac{\pi g}{2} \frac{1}{z-w} : \partial \psi(z) \partial \psi(w) : \\ &\sim \frac{1/4}{(z-w)^4} + \frac{2T(w)}{(z-w)^2} + \frac{\partial T(w)}{z-w}, \end{aligned}$$

thus proving that the free fermion has a central charge  $c = 1/2$ .

### 5.2.3 Entanglement entropy in a 1 + 1 dimensional strip

After Hawking's discovery of black hole radiation in 1975 [Haw75], the study of quantum effects and information exchange in black holes became a topic of intense study, and thus followed investigations on entropy in conformal field theory that have resurfaced for use in quantum information theory. Srednicki [Sre93] computed numerically the entropy of both 3 + 1 and 1 + 1 dimensional bosonic, massless models and identified the logarithmic divergence of the latter. Later, Callan and Wilzcek [CW94] came up with the concept of geometric entropy on a 1 + 1 dimensional conformal strip, which was pursued by Holzhey, Larsen and Wilzcek [HLW94]. The results have been generalized by Calabrese and Cardy to other geometries and finite temperature [CC04, Kor04], and also the time evolution of the entanglement has been investigated [CC05].

The analysis starts with a series of conformal transformations in the plane. Assume that the initial coordinate is  $z = x + i\tau$ , where  $x$  is the spatial coordinate and  $\tau$  is the time. The system is of length  $L$ , such that  $0 < x < L$ , and the subsystem we're interested in is  $0 < x < \ell$ . We denote the surfaces at  $\tau = 0$  as  $\mathcal{S}$  for the subsystem and  $\mathcal{C}$  for the entire system. Now, periodic boundary condition in  $x$  make this model an infinitely long cylinder of circumference  $L$ , the length of the system. The first conformal transformation is [HLW94]

$$\zeta = -\frac{\sin\left[\frac{\pi}{L}(z - \ell)\right]}{\sin\left(\frac{\pi z}{L}\right)}. \quad (5.8)$$

This maps  $\mathcal{C}$  onto the real axis, with  $\mathcal{S}$  as the negative half-axis and the rest  $\mathcal{S}' = \mathcal{C} \setminus \mathcal{S}$  as the positive axis. Moreover, the infinite past is a point in the upper half-plane,  $\zeta(\tau = -\infty) = -e^{-i\pi\ell/L}$ , and the infinite future is at the point  $\zeta(\tau = \infty) = -e^{i\pi\ell/L}$  in the lower half-plane. Next, we employ the transformation  $w = \frac{1}{\pi} \ln \zeta$ , which maps  $\mathcal{S}$  onto the real axis with  $x \rightarrow 0$  corresponding to  $w \rightarrow \infty$ , and  $x \rightarrow \ell^-$  corresponding to  $w \rightarrow -\infty$ . The remainder of the system is the line  $w = i$  with  $z \rightarrow \ell^+$  becoming  $w \rightarrow -\infty + i$ , and  $z \rightarrow L$  becoming  $w \rightarrow \infty + i$ . The infinite past and future maps to the points  $w(\tau = \pm\infty) = i(1 \pm \ell/L)$ . Both transformations  $z \rightarrow \zeta \rightarrow w$  are sketched in Figure 5.2.

Now, we can use the so-called replica trick to make the identification

$$S = -\text{Tr} \rho \log \rho = -\lim_{n \rightarrow 1} \frac{d}{dn} \text{Tr} \rho^n. \quad (5.9)$$

This assumes that integer values of  $n$  can be made into an analytical continuation for non-integer  $n$ . Thus the problem is reduced into computing  $\rho^n$  on the surface defined by  $w$ . The functional integral defining  $\rho$  is

$$\rho(\phi, \phi') = \int \mathcal{D}\chi |\phi, \chi\rangle \langle \phi', \chi|,$$

where  $\chi$  designates the fields on the upper line, while  $\phi$  are the fields on  $\mathcal{S}$ , that is the real axis. This integral is equivalent to cloning the strips  $\mathcal{C}$ , with the intersection along  $\mathcal{S}'$ , with boundary conditions specifying  $\phi$  and  $\phi'$ . Thus one gets a strip of width 2 to integrate along. Using functional integral representation of the wave function  $|\phi, \chi\rangle$  one finds that

$$\text{Tr} \rho^n = \frac{\mathcal{Z}(n)}{\mathcal{Z}(1)^n},$$

where  $\mathcal{Z}(n)$  is the path integral of the strip  $\mathcal{C}$  cloned  $n$  times such that one gets a structure of width  $2n$  and boundary conditions restricting the fields on the extremal surfaces. From this one finds the entropy (or entanglement entropy) to be [HLW94, CC04]

$$S \sim \frac{c + \bar{c}}{6} \log \left[ L \sin \left( \frac{\pi \ell}{L} \right) \right] \quad (5.10)$$



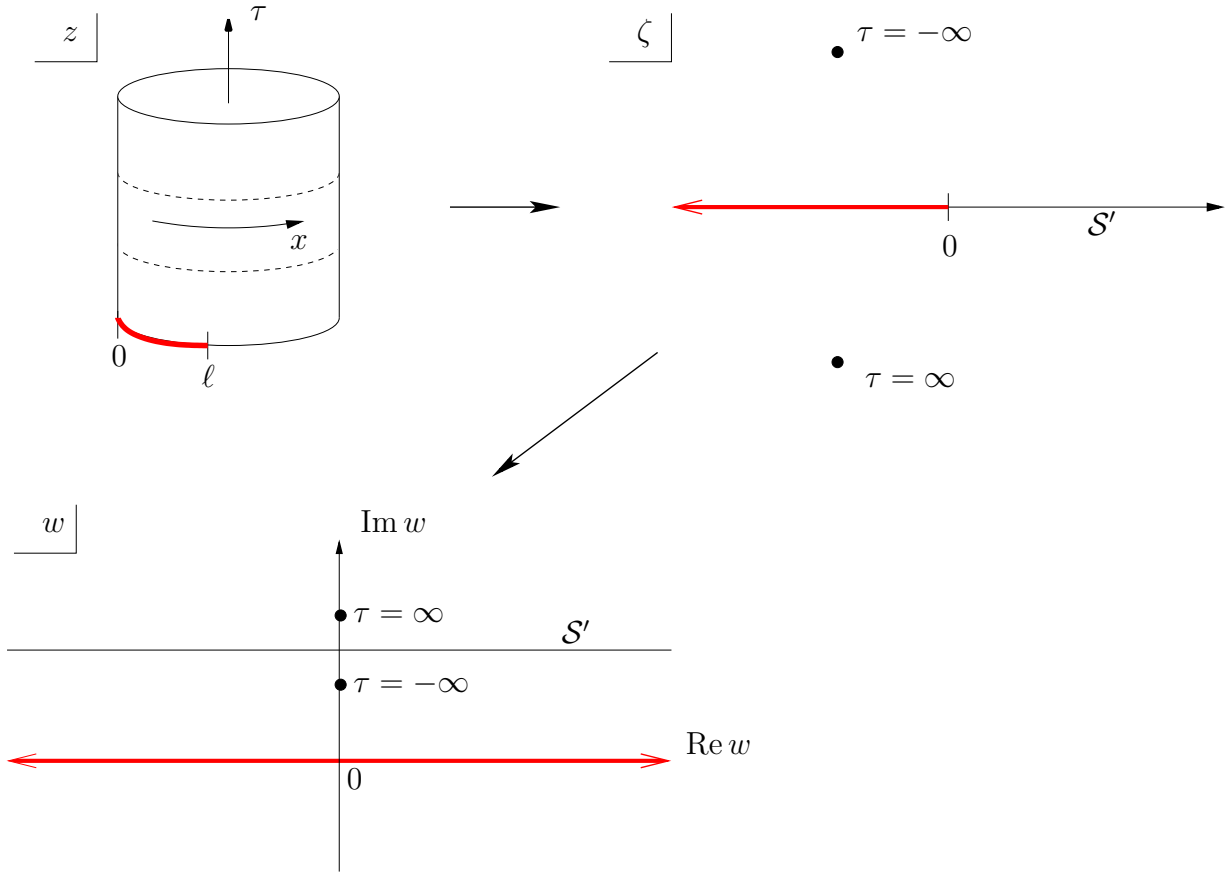


**Figure 5.2:** The conformal transformations described in the text,  $z \rightarrow \zeta$  defined by (5.8) and  $\zeta \rightarrow w = \frac{1}{\pi} \ln \zeta$ . The red arc indicates the system,  $\mathcal{S}$ .

where  $\sim$  indicates up to an additive constant independent of  $\ell$  and  $L$ . The derivation is valid in the limit  $\ell, L - \ell \gg a$  with  $a$  the lattice spacing of the model. The entropy is symmetric around  $\ell = L/2$ , at which point the entropy is largest. From this it is easy to see that for an (semi-)infinite system,  $L \rightarrow \infty$ , the entropy diverges logarithmically  $S \sim \frac{c+\bar{c}}{6} \log \ell$ . Also, when considering systems of different sizes  $L$ , with a constant fraction  $\ell/L$ , one also has a logarithmic divergence,  $S \sim \frac{c+\bar{c}}{6} \log L$ .

## 5.2.4 Conformal invariance in QPT

We expect conformal invariance at quantum critical points in  $1+1$  dimensional models due to the scale invariance that emerges here. It is reasonable to demand nearest-neighbor (or perhaps next nearest-neighbor) interaction to keep interactions local. Thus it is possible to identify a central charge to the quantum phase transition (QPT), and the central charge defines the corresponding Virasoro algebra. Hence it is, in principle, possible to identify the

critical exponents of the model according to the scaling dimensions of the fields. Friedan *et al.* [FQS84] proved that in models where the Virasoro algebra has unitary representation<sup>2</sup>, and  $c \leq 1$ , the central charge is restricted to the values

$$c = 1 - \frac{6}{m(m+1)} \quad m = 3, 4, \dots, \quad (5.11)$$

and for each value of  $c$  there are  $m(m-1)/2$  allowed values of  $h$  given by

$$h_{r,s}(m) = \frac{[(m+1)r - ms]^2 - 1}{4m(m+1)} \quad r = 1, \dots, m-1 \quad \text{and} \quad s = 1, \dots, p.$$

Moreover, each such value of  $c$  corresponds to a universality class (or a set of such), and for the first few values the mapping is shown in Table 5.1.

**Table 5.1:** The universality classes corresponding to the first allowed central charges  $c \leq 1$ . [FQS84, Gin89]

$m$	$c$	Universality class
3	$\frac{1}{2}$	Ising, free fermion
4	$\frac{7}{10}$	Tricritical Ising
5	$\frac{4}{5}$	3-state Potts
6	$\frac{6}{7}$	Tricritical 3-state Potts
$\vdots$	$\vdots$	
$\infty$	1	Free boson

It is remarkable that the conformal invariance at the critical point gives information about which universality class the model belongs to. There is a deep connection between the conformal invariance of the underlying structure and the statistical mechanics of the model, a feature that we will exploit in later chapters.

### 5.3 Quantum models

We will in this section present a limited number of quantum models which exhibits quantum phase transitions and describe some properties. In general, a spin-1/2 quantum chain with periodic boundary conditions has a Hamiltonian

$$H = - \sum_{n=1}^N \left[ \sum_{\alpha=x,y,z} f_{\alpha} \sigma_n^{\alpha} \sigma_{n+1}^{\alpha} + \mathbf{g} \cdot (\boldsymbol{\sigma}_n \times \boldsymbol{\sigma}_{n+1}) + \boldsymbol{\lambda} \cdot \boldsymbol{\sigma}_n \right], \quad (5.12)$$

<sup>2</sup>Such models are usually called *unitary models*, and are those where the representation of the Virasoro algebra contains no negative norm states. All such representations with  $c > 1$  (and  $h > 0$ ) are unitary.

where  $\mathbf{f}$ ,  $\mathbf{g}$ , and  $\boldsymbol{\lambda}$  are real 3-vectors, and  $\boldsymbol{\sigma}_{N+1} \equiv \boldsymbol{\sigma}_1$ . Further,  $\boldsymbol{\sigma}_n = (\sigma_n^x, \sigma_n^y, \sigma_n^z)$  are the conventional Pauli matrices. Fixing the coordinate system, this leaves us with seven degrees of freedom in the Hamiltonian, which is a huge parameter space to explore for phase transitions. The models with various parameters zero, or equal are usually known under a plethora of names. We will always consider  $\mathbf{g} = 0$ , and assume  $\boldsymbol{\lambda}$  to point in the positive  $z$ -direction,  $\boldsymbol{\lambda} = (0, 0, \lambda)$ . Still the model can be adjusted by a constant, so we can write down a general three parameter model, which we will denote the  $XYZ$  model;

$$H_{XYZ} = - \sum_n \left[ \sum_{\alpha} f_{\alpha} \sigma_n^{\alpha} \sigma_{n+1}^{\alpha} + \lambda \sigma_n^z \right] \quad \text{with} \quad f_x + f_y = 1. \quad (5.13)$$

When  $f_y = f_z = 0$  this is known as the quantum Ising model, and when  $f_y \geq 0$  we get the  $XY$  model, both of which will be discussed in detail shortly. In particular the critical  $XY$  model with  $f_x = f_y$  and  $f_z = \lambda = 0$  is sometimes known as the  $XX$  model [Wan01b]. When  $f_x = f_y = f_z \geq 0$  and  $\lambda \geq 0$  we have the  $XXX$  model or simply the 1D Heisenberg model [ABV01]. When  $\lambda = 0$  and  $\mathbf{f} > 0$  we get what is also sometimes known as the  $XYZ$  model, a model that in terms of transfer matrices can be considered equivalent to the classical eight-vertex model [Sut70]. In the same way, the case  $\lambda = 0$ ,  $f_x = f_y \geq 0$  and  $f_z \geq 0$  is known as the  $XXZ$  model, or in terms of the transfer matrix equivalent to the classical six-vertex model [Lie67, Wan01a], which in its quantum version has been suggested to describe the  $d$ -density wave competing with superconductivity in high- $T_C$  superconductors [Cha02, SC06]. Curiously, the model was in its early days considered for explaining “residual entropy” in ice at low temperatures [Lie67], which suggests the wide applicability of these models, not restricted to quantum mechanics. All these models investigated and some solved exactly, which makes them useful as benchmark tools. In particular, the Ising model is simple and intuitively easy to assess. The various models are not only mathematical playgrounds – though they are useful as such – but are also efficient models to simulate real life systems in addition to the examples already mentioned. E.g. the vertex models were originally conceived to model a second order polarization transition at 122 K in potassium dihydrogen phosphate,  $\text{KH}_2\text{PO}_4$  [Sla41].

### 5.3.1 The Ising model

The Ising model is perhaps the quantum model which is studied in greatest detail, and where most is known. Hence it makes for a good starting point for further studies. We investigate the quantum Ising model in one spatial dimension, whose Hamiltonian is

$$H_{\text{Ising}} = - \sum_{n=1}^N (\sigma_n^x \sigma_{n+1}^x + \lambda \sigma_n^z). \quad (5.14)$$

The  $\sigma$ s are the conventional Pauli spin matrices while  $\lambda$  is our external parameter, a magnetic field in the  $z$ -direction. Naïvely, one expects in the limit  $\lambda \rightarrow \infty$  all spins aligned

in the  $z$ -direction, which is a product state and thus has no entanglement. However, in the zero field limit, the ground state would have to be a Schrödinger cat state with a superposition between the spins in positive and negative  $x$ -direction respectively.

This 1D quantum model can be mapped onto the 2D classical Ising model, which Onsager famously solved in 1944 [Ons44]. The classical model has a continuous phase transition at a critical temperature  $T = T_c$ , which in the quantum case is mapped onto a critical magnetic field  $\lambda_c = 1$ .

In the  $\lambda \rightarrow 0$  limit we have unit entropy due to the one-qubit entanglement in the ground state, which is a Schrödinger cat state, while the large  $\lambda$  limit the product state means that the entropy falls to zero. However, we see that with larger system sizes there appears what seems to be a divergence at  $\lambda = 1$ . Even in small systems the entropy here is larger than elsewhere, but for larger systems the effect is more pronounced. Note that we need a large system (roughly  $N > 50$ ) to say with any confidence that there is a phase transition at  $\lambda = 1$ , which indeed is the thermodynamic solution to this system.

In Figure 5.3 the gap and ground state energy of the Ising model is shown, and the approach towards a gapless state as  $N \rightarrow \infty$  is clearly shown. Note also that the  $N = 10$  system is far from gapless, and one should therefore not anticipate much sign of the phase transition in this system, contrary to what shown in [SO05] and Section 5.4.5. Indeed, it is remarkable that even though a system of size of order 10 is far from gapless, and shows no critical properties, the conformal signature can still be very reliably used to identify the critical

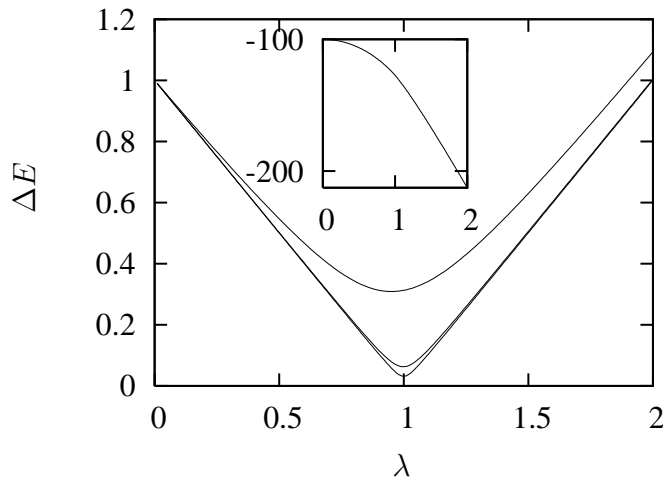


**Figure 5.3:** The gap  $\Delta E = \min_n \bar{\omega}_n$  between the ground state and first excited state energies in the Ising model with periodic boundary conditions. From top, the system sizes shown are  $N = 10, 50, 100$ . We see clearly that the system approaches a gapless state at the critical point  $\lambda = 1$  as the system size increases. The inset shows the ground state energy for the  $N = 100$  system.

parameters. The gap is here defined as  $\Delta E = \min_n \bar{\omega}_n$ , within the ground state parity segment.

### 5.3.2 The $XX$ model

The  $XX$  model in an external magnetic field is defined by the Hamiltonian

$$H_{XX} = - \sum_{n=1}^N (\sigma_n^x \sigma_{n+1}^x + \sigma_n^y \sigma_{n+1}^y + \lambda \sigma_n^z). \quad (5.15)$$

This model has a continuous  $U(1)$  symmetry in the  $xy$  plane, which by the Mermin-Wagner theorem [MW66] cannot be spontaneously broken at non-zero temperatures in two dimensions in classical systems. Thus, in quantum models in one dimension at zero temperature, no spontaneous symmetry breaking can occur. Nevertheless, polynomial decay of the correlation function may exist due to vortex excitations such as the Kosterlitz-Thouless transition in the classical  $XY$  model [KT73]. The parity operator  $\mathcal{P} = \bigotimes_k \sigma_k^z$  commutes with the Hamiltonian, and thus its eigenvalue, the parity  $\mathcal{P} = \pm 1$  is a good quantum number, and the solution space is split into two subspaces, as demonstrated in Section 3.1. In this model the generator of rotation,  $\mathcal{L} = \sum_n \sigma_n^z$  also commutes with the Hamiltonian, and its eigenvalue  $\hat{l}$  is thus also a good quantum number. In terms of the spin flip operators  $\sigma^\pm = (\sigma^x \pm i\sigma^y)/\sqrt{2}$ , the Hamiltonian can be rewritten

$$H_{XX} = - \sum_n (\sigma_n^+ \sigma_{n+1}^- + \sigma_n^- \sigma_{n+1}^+) - \lambda \mathcal{L}.$$

Obviously, the product states  $|N\rangle = |1\rangle^{\otimes N}$  and  $|-N\rangle = |0\rangle^{\otimes N}$  (labelled by their  $\hat{l}$  values) are the exact ground states in the limits  $\lambda \rightarrow \pm\infty$  respectively. More precisely, applying the Hamiltonian to these states yield  $H_{XX}|N\rangle = -\lambda N|N\rangle$  and  $H_{XX}|-N\rangle = \lambda N|-N\rangle$ , showing that the state  $|N\rangle$  has lower energy of these two when  $\lambda > 0$ . However, it is not obvious that these states are the ground states for all  $\lambda$ . The parities of the states are  $p(|N\rangle) = 1$  and  $p(|-N\rangle) = (-1)^N$ .

Consider the simplest “excitations” to the state  $|N\rangle$ , the  $N$  states

$$|N-2, m\rangle = |1\rangle^{\otimes(m-1)} \otimes |0\rangle \otimes |1\rangle^{\otimes(N-m)} \quad m = 1, \dots, N.$$

Applying the Hamiltonian to this state gives

$$H_{XX}|2-N, m\rangle = - [|N-2, m-1\rangle + |N-2, m+1\rangle + \lambda(N-2)|2-N, m\rangle].$$

Thus, it is not an eigenstate of the Hamiltonian, but we can define a translationally invariant state, or a spin-wave state

$$|N-2, k\rangle = \frac{1}{\sqrt{N}} \sum_m e^{2\pi i k m / N} |N-2, m\rangle, \quad k = 1, \dots, N,$$

which diagonalizes the Hamiltonian. That is,

$$H_{XX}|N-2, k\rangle = \left[ -\lambda N + 2 \left( \lambda - \cos \frac{2\pi k}{N} \right) \right] |N-2, k\rangle. \quad (5.16)$$

The excitation energy of the spin-wave state compared to the product state  $|N\rangle$  is  $\Delta E = +2 \left( \lambda - \cos \frac{2\pi k}{N} \right)$ , which may be negative when  $\lambda < 1$ . Likewise, we can define the simplest excitation to the state  $|-N\rangle$  as

$$|-N+2, m\rangle = |0\rangle^{\otimes(m-1)} \otimes |1\rangle \otimes |0\rangle^{\otimes(N-m)} \quad m = 1, \dots, N,$$

and the corresponding spin-wave state  $|-N+2, k\rangle$ , which diagonalizes the Hamiltonian and has energy eigenvalues

$$H_{XX}|-N+2, k\rangle = \left[ \lambda N - 2 \left( \lambda + \cos \frac{2\pi k}{N} \right) \right] |-N+2, k\rangle. \quad (5.17)$$

Here, the excitation energy is  $\Delta E = -2 \left( \lambda + \cos \frac{2\pi k}{N} \right)$ , which can be negative when  $\lambda > -1$ . Thus, the ground state is shown to be  $|N\rangle$  when  $\lambda > 1$  and  $|-N\rangle$  when  $\lambda < -1$ , while the ground state in the intermediate region is undetermined.

## 5.4 The XY model

The XY model is a simple generalization of the Ising and XX models, conventionally written

$$H_{XY} = - \sum_n \left( \frac{1+\gamma}{2} \sigma_n^x \sigma_{n+1}^x + \frac{1-\gamma}{2} \sigma_n^y \sigma_{n+1}^y + \lambda \sigma_n^z \right), \quad (5.18)$$

where  $\gamma = 1$  is the Ising model and  $\gamma = 0$  the XX model already discussed. First properly solved by Barouch and McCoy [BM71] this is now a thoroughly investigated model [Ort05, ON02a] which is useful for benchmarking due to its simplicity and still rich structure. A schematic phase diagram of the model is presented in Figure 5.4. A simple assessment of the model shows that the ground state in the large field limit where  $\lambda \rightarrow \infty$  is the pure state  $|\Omega_z\rangle = |\uparrow\rangle^{\otimes N}$ . In the low field, when  $\gamma > 0$ , the ground state will be the Schrödinger cat state with positive and negative  $x$  direction being equivalent,  $|\Omega_x\rangle = (|\rightarrow\rangle^{\otimes N} + |\leftarrow\rangle^{\otimes N})/\sqrt{2}$ . Finally, for negative  $\gamma$  the ground state will be the Schrödinger cat state with superpositions in the  $y$  direction,  $|\Omega_y\rangle = (|\nearrow\rangle^{\otimes N} + |\swarrow\rangle^{\otimes N})/\sqrt{2}$ . Here vertical arrows indicate eigenstates of  $\sigma^z$ , horizontal arrows eigenstates of  $\sigma^x$  and diagonal arrows eigenstates of  $\sigma^y$ . Strictly speaking these assessments are only valid in the extreme limits, but one can assume that they are reasonably close to the actual states also in some region away from these limits. In the thermodynamic limit one can assume this to be the case arbitrarily close to the phase transition.

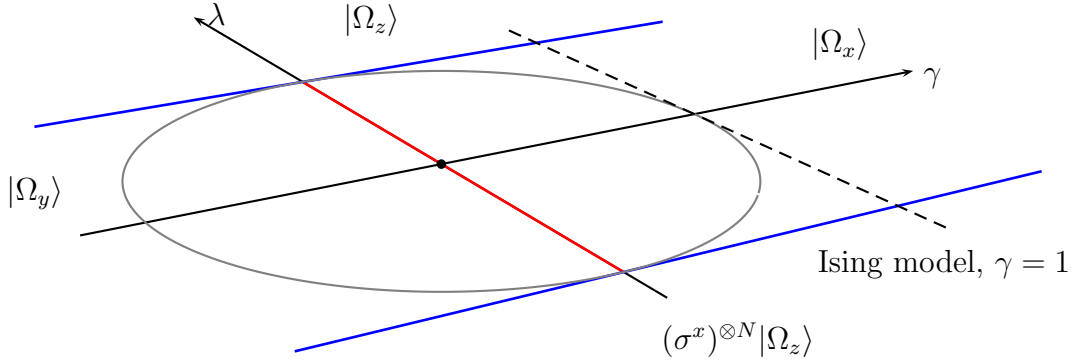


**Figure 5.4:** The phase diagram of the  $XY$  model as defined in (5.18). The blue lines indicate the phase transition between the pure state with spins aligned in the  $z$  direction and the Schrödinger cat states. The red separates the Schrödinger cat state in  $\pm x$  direction from  $\pm y$  direction. The circle indicates the BM-circle.

Barouch and McCoy also acknowledged the existence of the unit circle  $\gamma^2 + \lambda^2 = 1$  as the division line between what they denoted the oscillatory region inside the circle and monotonic region outside due to the behavior of the  $xx$  correlation function in the large distance limit [BM71]. However, this is not considered a true phase transition, but rather a boundary region. The three phases of the model have been denoted ordered oscillatory ( $\gamma^2 + \lambda^2 < 1$ ), ordered ferromagnetic ( $\gamma^2 + \lambda^2 > 1$  and  $|\lambda| < 1$ ) and paramagnetic ( $|\lambda| > 1$ ) [WDM<sup>+</sup>05]. At this so-called BM-circle after its discoverers, the entanglement entropy is always unity [LLRV05].

### 5.4.1 Fermionization

One of the reasons for the feasibility of the  $XY$  model is that it can be mapped onto a string of spinless fermions, using the technique of a Jordan-Wigner transform. This reduces the dimensionality of the problem from the  $2^N \times 2^N$  matrices of the spin formulation to  $2N \times 2N$  sized matrices. The technique can be applied more generally, but we will demonstrate it on the  $XY$  model here.

We apply a Jordan-Wigner transform that introduces fermionic operators  $a_n$  and  $a_n^\dagger$

$$a_n = \frac{1}{2} \left( \bigotimes_{k=1}^{n-1} \sigma_k^z \right) \otimes (\sigma_n^x + i\sigma_n^y) \quad a_n^\dagger = \frac{1}{2} \left( \bigotimes_{k=1}^{n-1} \sigma_k^z \right) \otimes (\sigma_n^x - i\sigma_n^y), \quad (5.19)$$

which ensures the anti-commutation of these operators,

$$\{a_n, a_m^\dagger\} = \delta_{nm} \quad \{a_n, a_m\} = 0.$$

The spin operators can be expressed in terms of these fermion operators as

$$\sigma_n^z = 2a_n a_n^\dagger - \mathbb{1} \quad (5.20)$$

$$\begin{bmatrix} \sigma_n^x \sigma_{n+1}^x \\ \sigma_n^x \sigma_{n+1}^y \\ \sigma_n^y \sigma_{n+1}^x \\ \sigma_n^y \sigma_{n+1}^y \end{bmatrix} = \begin{bmatrix} -1 & -1 & 1 & 1 \\ i & -i & -i & i \\ i & i & i & i \\ 1 & -1 & 1 & -1 \end{bmatrix} \begin{bmatrix} a_n a_{n+1} \\ a_n a_{n+1}^\dagger \\ a_n^\dagger a_{n+1} \\ a_n^\dagger a_{n+1}^\dagger \end{bmatrix}. \quad (5.21)$$

In turn, this means that the Hamiltonian can be written as a sum of quadratic fermion operators, which in general is

$$H = A_{mn}(a_m^\dagger a_n - a_m a_n^\dagger) + B_{mn} a_m^\dagger a_n^\dagger - B_{mn}^* a_m a_n$$

with  $A$  and  $B$  being  $N \times N$  matrices where  $A$  is real and symmetric. In the special case of the  $XY$  model these parameter matrices become

$$A = \begin{bmatrix} \lambda & -\frac{1}{2} & 0 & & \\ -\frac{1}{2} & \lambda & -\frac{1}{2} & & \\ 0 & -\frac{1}{2} & \lambda & -\frac{1}{2} & \\ & 0 & -\frac{1}{2} & \lambda & \\ & & & & \ddots \end{bmatrix} \quad B = \frac{1}{2}\gamma \begin{bmatrix} 0 & -1 & 0 & & \\ 1 & 0 & -1 & 0 & \\ 0 & 1 & 0 & -1 & \\ & 0 & 1 & 0 & \\ & & & & \ddots \end{bmatrix}. \quad (5.22)$$

The above holds for the case of open boundary conditions, where the sum in (5.18) goes from 1 to  $N - 1$ . However, for the case of periodic boundary conditions, the upper limit of the sum is  $N$ , and by definition  $\sigma_{N+1} \equiv \sigma_1$ . For this case we must utilize the parity operator  $\mathcal{P} = \bigotimes_{k=1}^N \sigma_k^z$ , which commutes with the Hamiltonian, and  $a_N a_1 = -\sigma_N^+ \sigma_1^- \mathcal{P}$ .<sup>3</sup> Also, for generality one can assume that the chain is non-homogeneous, such that the  $\lambda$  and  $\gamma$ s are local,  $\{\lambda_n\}$  and  $\{\gamma_n\}$ . For the case of the  $A$  and  $B$  matrices above, they now become

$$A = \begin{bmatrix} \lambda_1 & -\frac{1}{2} & 0 & \cdots & \frac{1}{2}\mathcal{P} \\ -\frac{1}{2} & \lambda_2 & -\frac{1}{2} & & 0 \\ 0 & -\frac{1}{2} & \lambda_3 & & 0 \\ \vdots & & & \ddots & \vdots \\ \frac{1}{2}\mathcal{P} & 0 & 0 & \cdots & -\frac{1}{2} & \lambda_N \end{bmatrix} \quad B = \frac{1}{2} \begin{bmatrix} 0 & -\gamma_1 & 0 & \cdots & 0 & -\gamma_N \mathcal{P} \\ \gamma_1 & 0 & -\gamma_2 & & 0 & 0 \\ 0 & \gamma_2 & 0 & & & 0 \\ \vdots & & & \ddots & & \vdots \\ 0 & & & & & -\gamma_{N-1} \\ \gamma_N \mathcal{P} & 0 & 0 & \cdots & \gamma_{N-1} & 0 \end{bmatrix}. \quad (5.23)$$

<sup>3</sup>To see this, use direct computation and the fact that  $\sigma^\pm = \mp \sigma^\pm \sigma^z$ .



Replacing homogeneous parameters and a virtual parity  $\mathcal{P} = 0$ , we recover Eq. (5.22). Hence, the open boundary conditions can easily be recovered from the equations for periodic boundary conditions by setting  $\mathcal{P} = 0$ .

For the homogeneous, closed chain we thus obtain

$$H_{XY} = \frac{1}{2} \sum_{n=1}^N \left[ a_n a_{n+1}^\dagger - a_n^\dagger a_{n+1} + \gamma \left( a_n a_{n+1} - a_n^\dagger a_{n+1}^\dagger \right) + \lambda \left( a_n^\dagger a_n - a_n a_n^\dagger \right) \right] \quad (5.24)$$

where we must interpret  $a_N a_{N+1} \equiv -a_N a_1 \mathcal{P}$ . Now, considering the positive parity subspace,  $\mathcal{P} = 1$ , the boundary condition in terms of the fermions become anti-periodic, and we can expand the field in an anti periodic Fourier series of new fermionic operators  $b_k$  and  $b_k^\dagger$ :

$$a_n = \frac{1}{\sqrt{N}} \sum_{k=1}^N b_k e^{\pi i (2k+1)n/N}, \quad a_n^\dagger = \frac{1}{\sqrt{N}} \sum_{k=1}^N b_k^\dagger e^{-\pi i (2k+1)n/N}.$$

In terms of these, the positive parity Hamiltonian  $H_{XY}^{(+)}$  becomes

$$H_{XY}^{(+)} = \sum_{k=1}^N \left[ \left( \cos \frac{\pi(2k+1)}{N} - \lambda \right) \left( b_k b_k^\dagger - b_k^\dagger b_k \right) + i\gamma \sin \frac{\pi(2k+1)}{N} \left( b_{-k} b_k - b_k^\dagger b_{-k}^\dagger \right) \right].$$

We have used the convention that  $-k \equiv N - k - 1$ . Next, we use a Bogoliubov transformation to diagonalize the Hamiltonian,

$$\begin{bmatrix} i b_k \\ -i b_{-k}^\dagger \end{bmatrix} = \begin{bmatrix} \cos \phi_k & -\sin \phi_k \\ \sin \phi_k & \cos \phi_k \end{bmatrix} \begin{bmatrix} c_k \\ c_{-k}^\dagger \end{bmatrix}$$

where the parameter  $\phi_k$  is assumed to fulfill  $\phi_{-k} = -\phi_k$  and  $c_k, c_k^\dagger$  are new fermion operators. For brevity, we define  $\alpha_k = \frac{\pi(2k+1)}{N}$ , and get

$$H_{XY}^{(+)} = \sum_k \left\{ [(\cos \alpha_k - \lambda) \cos 2\phi_k - \gamma \sin \alpha_k \sin 2\phi_k] \left( c_k c_k^\dagger - c_k^\dagger c_k \right) + [(\cos \alpha_k - \lambda) \sin 2\phi_k + \gamma \sin \alpha_k \cos 2\phi_k] \left( c_{-k} c_k + c_k^\dagger c_{-k}^\dagger \right) \right\}.$$

This becomes diagonal upon choosing

$$\cos 2\phi_k = \frac{\lambda - \cos \alpha_k}{\mathcal{N}_k} \quad \text{and} \quad \sin 2\phi_k = \frac{\gamma \sin \alpha_k}{\mathcal{N}_k},$$

with

$$\mathcal{N}_k^2 = (\lambda - \cos \alpha_k)^2 + \gamma^2 \sin^2 \alpha_k.$$

Note that the condition  $\phi_{-k} = -\phi_k$  is fulfilled. This finally means that the Hamiltonian becomes

$$H_{XY}^{(+)} = \sum_{k=1}^N \underbrace{\sqrt{(\lambda - \cos \alpha_k)^2 + \gamma^2 \sin^2 \alpha_k}}_{\Omega_k} \left( 2c_k^\dagger c_k - 1 \right). \quad (5.25)$$

The same procedure can be applied to the negative parity subspace, only now with periodic boundary conditions and periodic Fourier series,

$$a_n = \frac{1}{\sqrt{N}} \sum_{k=1}^N \hat{b}_k e^{2\pi i k n / N},$$

and we arrive at (5.25) with  $\alpha_k = 2\pi k / N$  and corresponding new fermion operators. In Figure 5.5 the energy eigenvalues is plotted with  $\alpha_k$ , for various parameters, and we see clearly that the critical points correspond to zeros in the energy gap.

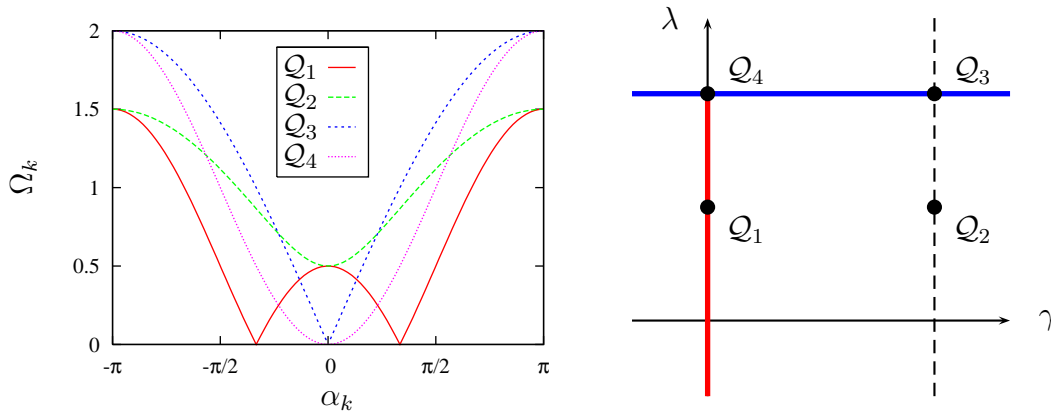


**Figure 5.5:** *Left:* The energy modes  $\Omega_k$  are shown for the four points in the phase space  $(\gamma, \lambda)$ ;  $Q_1 = (0, 0.5)$ ,  $Q_2 = (1, 0.5)$ ,  $Q_3 = (1, 1)$ , and  $Q_4 = (0, 1)$ .

*Right:* The points shown designated in the phase space of the XY model.

The parity of the ground state is important when investigating small systems — for large systems the difference is minute — in order to know which subspace to look for the ground state. This is not a trivial question, and we resort to direct computation of the two subspaces, and check which yields the lowest ground state energy. Brute computation shows that when  $\gamma^2 + \lambda^2 > 1$ , that is outside the BM-circle, the ground state parity is always positive<sup>4</sup>. Inside the BM-circle, the nature of the ground state is oscillatory, and the parity of the ground state in a  $N = 10$  system is shown in Figure 5.6. The BM-circle limits the outer region of the circle, and the oscillatory nature of the ground state inside the circle is shown. When the system size increases the difference between the ground state in the different parity subspaces become negligible.

## 5.4.2 Diagonalization in terms of Majorana fermions

Having established the fermionic shape of the Hamiltonian in question, which in this case is the XY model, and which take on the form of the two matrices  $A$  and  $B$ , we must

<sup>4</sup>When  $N$  is odd, it will be negative outside this circle for negative  $\lambda$ . We consider only even  $N$  in the following.

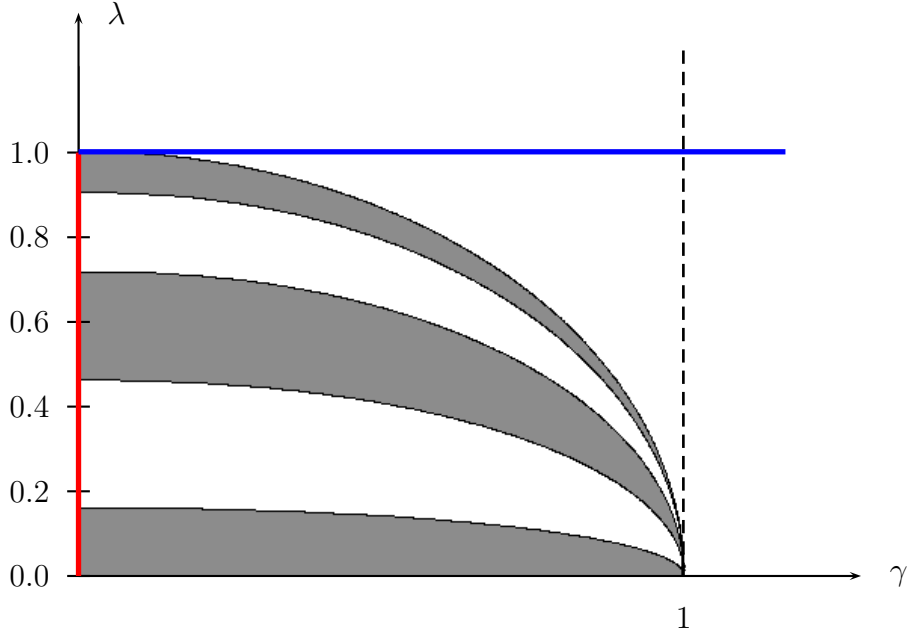


**Figure 5.6:** The areas in the first quadrant of the parameter space of the  $XY$  model where the ground state has negative parity are shaded for an  $N = 10$  system. The outermost line coincides precisely with the BM circle  $\gamma^2 + \lambda^2 = 1$ . The critical lines and the Ising line (dashed) is drawn for reference.

diagonalize the Hamiltonian. To this end, define the  $2N$  Majorana fermions in terms of the operators

$$\tilde{\gamma}_{2i-1} = \frac{1}{i\sqrt{2}}(a_i - a_i^\dagger) \quad \tilde{\gamma}_{2i} = \frac{1}{\sqrt{2}}(a_i + a_i^\dagger). \quad (5.26)$$

These operators satisfy the Majorana anti-commutation relations  $\{\tilde{\gamma}_i, \tilde{\gamma}_j\} = \delta_{ij}$ . Moreover, in terms of these operators the Hamiltonian becomes

$$H = \mathcal{C}_{ij} \tilde{\gamma}_i \tilde{\gamma}_j,$$

where the Hermitian matrix  $\mathcal{C}$  is

$$\mathcal{C} = i \begin{bmatrix} \Xi_{11} & \Xi_{12} & \cdots \\ \Xi_{21} & \Xi_{22} & \\ \vdots & & \ddots \end{bmatrix} \quad \Xi_{mn} \equiv \begin{bmatrix} -\text{Im } B_{mn} & -(A_{mn} + \text{Re } B_{mn}) \\ A_{mn} - \text{Re } B_{mn} & \text{Im } B_{mn} \end{bmatrix}.$$

$\mathcal{C}$  being imaginary and antisymmetric means that its eigenvalues are real and come in positive/negative pairs, which we denote  $\pm\bar{\omega}_n$ . The eigenvectors corresponding to such a pair are complex conjugates. In turn we now diagonalize  $\mathcal{C}^2$  with the orthogonal and real matrix  $O$ ,

$$O^T \mathcal{C}^2 O = \bigoplus_{n=1}^N \begin{bmatrix} \bar{\omega}_n^2 & 0 \\ 0 & \bar{\omega}_n^2 \end{bmatrix}.$$

If we are careful in permuting the columns of  $O$ , we can block diagonalize  $\mathcal{C}$  such that

$$O^T \mathcal{C} O = \bigoplus_{n=1}^N \begin{bmatrix} 0 & -i\bar{\omega}_n \\ i\bar{\omega}_n & 0 \end{bmatrix}.$$

Now we can return to fermions again, defining the  $N$  fermionic operators

$$\hat{a}_n = \frac{1}{\sqrt{2}} \sum_{i=1}^{2N} \check{\gamma}_i (O_{i,2n-1} + iO_{i,2n}) \quad (5.27)$$

$$\hat{a}_n^\dagger = \frac{1}{\sqrt{2}} \sum_{i=1}^{2N} \check{\gamma}_i (O_{i,2n-1} - iO_{i,2n}). \quad (5.28)$$

These diagonalize the Hamiltonian, such that

$$H = \sum_{n=1}^N \bar{\omega}_n (\hat{a}_n^\dagger \hat{a}_n - \hat{a}_n \hat{a}_n^\dagger). \quad (5.29)$$

Hence it is clear that the eigenstates of the Hamiltonian will be states with a defined number of  $\hat{a}$ -fermions. How this maps back to the real space fermions — never mind the spins — is far from trivial though. Nevertheless, it is clear that the ground state is the one with zero  $\hat{a}$  fermions. Any state in this basis we denote  $|\eta\rangle = |n_1, n_2, \dots, n_N\rangle$  where  $\eta$  is the set of fermionic occupation numbers and  $n_k = 0, 1$ .

This shows how the orthogonal matrix  $O$  plays a crucial role in diagonalizing the Hamiltonian, and that the new Hamiltonian is diagonal in terms of quasi-fermions related to the original fermions through the Bogoliubov transformation

$$\hat{a}_m = \Sigma_{mn} a_n + \Delta_{mn} a_n^\dagger \quad \hat{a}_m^\dagger = \Delta_{mn}^* a_n + \Sigma_{mn}^* a_n^\dagger \quad (5.30)$$

where the transformation matrices are

$$\Sigma_{mn} = \frac{1}{2} [O_{2n,2m-1} + O_{2n-1,2m} + i(O_{2n,2m} - O_{2n-1,2m-1})]$$

$$\Delta_{mn} = \frac{1}{2} [O_{2n,2m-1} - O_{2n-1,2m} + i(O_{2n,2m} + O_{2n-1,2m-1})].$$

Preservation of commutation relations and unitarity of the transformation ensure the following properties of the matrices  $\Sigma = \{\Sigma_{mn}\}$  and  $\Delta = \{\Delta_{mn}\}$ ,

$$\Sigma \Sigma^\dagger + \Delta \Delta^\dagger = \mathbf{1} \quad (5.31a)$$

$$\Sigma^\dagger \Sigma + \Delta^T \Delta^* = \mathbf{1} \quad (5.31b)$$

$$\Sigma \Delta^T + \Delta \Sigma^T = \mathbf{0} \quad (5.31c)$$

$$\Sigma^\dagger \Delta + \Delta^T \Sigma^* = \mathbf{0} \quad (5.31d)$$

Hence, when transforming from real fermions to the quasi-fermions, we apply the columns of  $O$ , where for each particle labeled  $n$ , two columns of  $O$  contribute, and every second term in this column contributes at a time. There is as we see a complex structure of the orthogonal matrix that creates the quasi-fermions. In general, the ground state of the Hamiltonian (5.29) will be  $|000\cdots 0\rangle$  in terms of the quasi-fermions, while it is not obvious how this can be mapped back to the real fermions. Nevertheless, this provides us with an easy manner in which we can find the properties of the ground state, such as the entropy.

The following argument ensures that we are able to diagonalize the basis we are working in, based on a matrix notation of (5.30),

$$\begin{bmatrix} \hat{\mathbf{a}} \\ \hat{\mathbf{a}}^\dagger \end{bmatrix} = \begin{bmatrix} \Sigma & \Delta \\ \Delta^* & \Sigma^* \end{bmatrix} \begin{bmatrix} \mathbf{a} \\ \mathbf{a}^\dagger \end{bmatrix}.$$

Here,  $\mathbf{a}$  is a column vector consisting of the  $a_n$ 's, while  $\mathbf{a}^\dagger$  is a column vector consisting of  $a_n^\dagger$ , not the adjoint of  $\mathbf{a}$ . We can diagonalize the matrices  $\Sigma\Sigma^\dagger$  and  $\Delta\Delta^\dagger$  simultaneously, since they commute by equation (5.31a). Hence, we can write

$$\Sigma\Sigma^\dagger = \mathbf{U}\mathbf{D}_\Sigma^2\mathbf{U}^\dagger \quad \text{and} \quad \Delta\Delta^\dagger = \mathbf{U}\mathbf{D}_\Delta^2\mathbf{U}^\dagger,$$

$\mathbf{U}$  being unitary and  $\mathbf{D}_{\Sigma|\Delta}^2$  are diagonal. Precisely likewise, we can do the same for the matrices involved in (5.31b),

$$\Sigma^\dagger\Sigma = \mathbf{V}\mathbf{D}_\Sigma^2\mathbf{V}^\dagger \quad \text{and} \quad \Delta^\dagger\Delta = (\Delta^\dagger\Delta)^* = \mathbf{V}\mathbf{D}_\Delta^2\mathbf{V}^\dagger,$$

$\mathbf{V}$  being another unitary matrix. The eigenvalues are however the same. Now, in order to preserve the two latter conditions in 5.31 we must have

$$\{\mathbf{D}_\Delta, \mathbf{D}_\Sigma\} = 0.$$

This can be accomplished since we have double degeneracy in both matrices by making these matrices  $2 \times 2$  block diagonal with two different Pauli matrices along the diagonal,

$$\mathbf{D}_\Sigma = \bigoplus_{k=1}^{N/2} \cos \vartheta_k \sigma^z \quad \text{and} \quad \mathbf{D}_\Delta = \bigoplus_{k=1}^{N/2} \sin \vartheta_k e^{i\chi_k} \sigma^y.$$

These will be diagonal when squared, and thus comply with the conditions above. We have assumed that the two degenerate terms are coincidental, if not the matrices can be rearranged to conform with this. If  $N$  is odd, one will have to add a single term along the diagonal consisting of a 0 (1) for the  $\mathbf{D}_\Sigma$  ( $\mathbf{D}_\Delta$ ). This procedure will ensure that the Bogoliubov transformation can be written

$$\begin{bmatrix} \hat{b}_{2n-1} \\ \hat{b}_{2n}^\dagger \end{bmatrix} = \begin{bmatrix} \cos \vartheta_n & -i \sin \vartheta_n e^{i\chi_n} \\ -i \sin \vartheta_n e^{-i\chi_n} & -\cos \vartheta_n \end{bmatrix} \begin{bmatrix} b_{2n-1} \\ b_{2n}^\dagger \end{bmatrix} \quad (5.32)$$

where the operators are unitarily transformed,

$$\hat{b}_n = \sum_k (U^{-1})_{nk} \hat{a}_k \quad b_n = \sum_k V_{nk} a_k. \quad (5.33)$$

Hence we have shown that the diagonalization can be accomplished through the unitary transformation (5.33) and Bogoliubov transformation (5.32).

### 5.4.3 Entropy in the $XY$ model

Having defined the  $XY$  model and how to diagonalize it, we now proceed to find the entropy of the ground state as described in section 2.1. As mentioned, the ground state is  $|00\cdots 0\rangle$  in terms of the delocalized quasi-fermions. We define the correlation matrix of the Majorana fermions

$$\Gamma_{ij} = \langle \tilde{\gamma}_i \tilde{\gamma}_j - \tilde{\gamma}_j \tilde{\gamma}_i \rangle. \quad (5.34)$$

Note that the Majorana fermions have a two-to-one correspondence to the real fermions, so tracing out a real fermion would amount to tracing out two neighbouring Majorana fermions from this matrix. In the  $\hat{a}$ -basis the correlator becomes

$$\Gamma_{ij} = \frac{i}{2} \sum_{k=1}^N (O_{i,2k} O_{j,2k-1} - O_{i,2k-1} O_{j,2k}).$$

So far we have considered the entire system, which is in a pure state, and the entropy is obviously zero unless we trace out some of the system leaving us with  $N' \leq N$  particles in the subsystem. Formally, this amounts to tracing out the two columns of  $\Gamma$  corresponding to these particles. Now, the density matrix is assumed diagonal in some quasi-fermion basis denoted  $\hat{a}$ . Note that this basis is different depending on the size (or shape) of the system traced out, but when nothing is traced out, it coincides with the basis that diagonalizes the Hamiltonian. Assume that in this basis the density operator can be written

$$\rho = \sum_{\eta} \Lambda_{\eta} |\eta\rangle \langle \eta| \quad \Lambda_{\eta} = \prod_{k=1}^{N'} [(1 - n_k) \lambda_k + n_k (1 - \lambda_k)] \quad (5.35)$$

where  $\eta$  denotes the set of fermionic occupation numbers  $\{n_1, n_2, \dots, n_{N'}\}$  of the quasi-fermions, and  $\lambda_k \in [0, 1]$  are real coefficients. The sum is over all possible occupation numbers,  $\sum_{\eta} = \sum_{n_1=0}^1 \cdots \sum_{n_{N'}=0}^1$ . Moreover, the ground state  $\rho = |0\rangle \langle 0|$  is identified by all  $\lambda_k = 1$ . Computing the expectation value matrix (5.34) in the  $\hat{a}$  basis we find that the matrix can be written

$$\Gamma_{ij} = \sum_{\eta} \Lambda_{\eta} \langle \eta | [\tilde{\gamma}_i, \tilde{\gamma}_j] | \eta \rangle = i \sum_{k=1}^{N'} (O_{i,2k} O_{j,2k-1} - O_{i,2k-1} O_{j,2k}) \left( \lambda_k - \frac{1}{2} \right),$$

and in turn this means that the transformation  $O$  block-diagonalizes this matrix;

$$O^T \Gamma O = i \bigoplus_{k=1}^{N'} \begin{bmatrix} 0 & -\lambda_k + \frac{1}{2} \\ \lambda_k - \frac{1}{2} & 0 \end{bmatrix}.$$

This shows that the eigenvalues of  $\Gamma$  are  $\pm (\lambda_k - \frac{1}{2})$ . The idea of this exercise is that given the diagonalization of the Hamiltonian, the matrix  $\Gamma$  is known, and the eigenvalues can

be numerically extracted efficiently even after tracing out some particles. Knowing the  $\lambda_k$ 's means that we know the density matrix, and can compute the entropy. The entropy becomes

$$S = - \sum_{\eta} \Lambda_{\eta} \log_2 \Lambda_{\eta} = \sum_{k=1}^{N'} H(\lambda_k) \quad (5.36)$$

where  $H(x)$  is the binary entropy (2.4). This gives us an efficient way to compute the entropy of any block of real spins through the transformation into quasi-fermions. Also the formulas here gives an easy relation between the *classical* entropy of the eigenvalues of the density matrix in the reduced  $\hat{a}$  basis and the entropy of the state itself. Figure 5.7 shows the entropy of the XY model when half-size is traced out. The entropy clearly has maxima along critical lines, while the actual height of the maximum is larger along the  $\gamma = 0$ -line than the  $\lambda = 1$ -line due to the larger central charge of this transition.

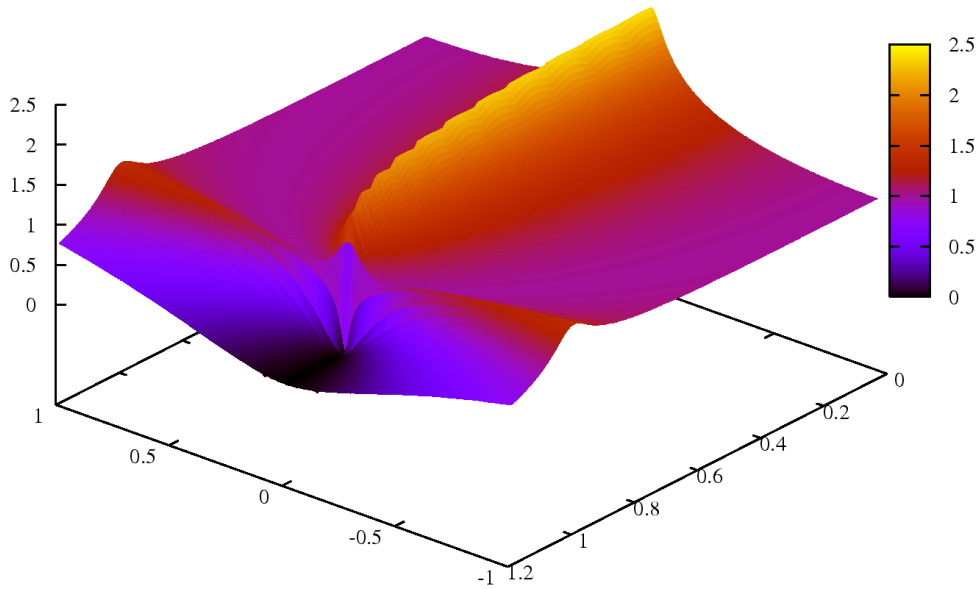


**Figure 5.7:** Entropy of the XY model when half of the spins are traced out. The critical lines  $\gamma = 0$  and  $\lambda = 1$  are seen as areas of increased entanglement. Here  $N = 50$ .

### 5.4.4 Other correlators

When we have established the matrices  $\Sigma$  and  $\Delta$  in the Bogoliubov transformation (5.30), we can compute expectation values and correlators of the model in question. Specifically, the second moment of annihilation and creation operators is

$$\langle \eta | a_n a_n^\dagger | \eta \rangle = \sum_{k=1}^{N'} [n_k |\Delta_{kn}|^2 + (1 - n_k) |\Sigma_{kn}|^2],$$

and hence follows e.g. the spin expectation value in the  $z$ -direction;

$$\langle \sigma_n^z \rangle = \sum_{\eta} \Lambda_{\eta} (2 \langle \eta | a_n a_n^\dagger | \eta \rangle - 1) = \sum_{k=1}^{N'} [\lambda_k |\Sigma_{kn}|^2 + (1 - \lambda_k) |\Delta_{kn}|^2].$$

Some more effort gives the fourth momenta, which enables us to compute the spin-spin correlation function,

$$s(k, l) \equiv \langle \sigma_k^z \sigma_l^z \rangle - \langle \sigma_k^z \rangle \langle \sigma_l^z \rangle.$$

This correlation will, when the distance  $|k - l|$  is sufficiently large, fall off exponentially, and the correlation length  $\xi$  is the cutoff of this exponential,  $s(k, l) \sim e^{-|k-l|/\xi}$ . Hence we find the correlation length in the Ising model as shown in figure 5.8. The correlation function follows the expected path nicely, though there obviously is no true divergence since the system size is finite.

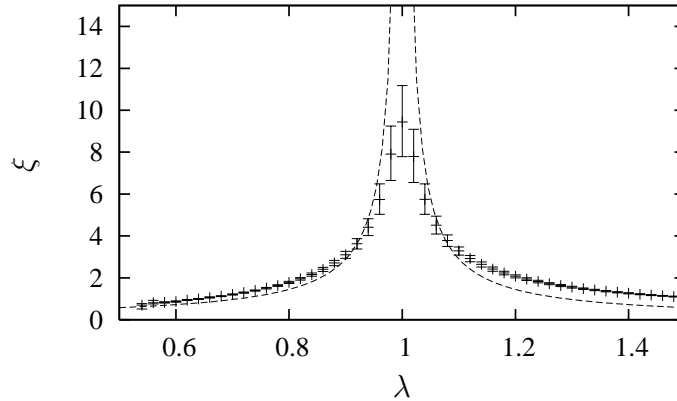


**Figure 5.8:** An estimate of the correlation length in the Ising model with magnetic field. The phase transition at  $\lambda = 1$  is clearly shown as a divergence in the correlation length. The error bars indicate the variation of the estimate of the correlation length, thus small error bars indicate a good approximation to exponential decay, while the large error bars close to the critical point reflect the polynomial decay here. The dashed line is the thermodynamical approximation  $\xi \sim |\lambda - \lambda_c|^{-1}$ . Data for  $N = 100$ .



The framework provided so far gives a good overview of the methods that can be utilized to find specific information about a large class of models. Nevertheless, there is an even larger class of models that do not conform to this framework, and where different approaches to finding the properties of the model has to be found.

### 5.4.5 Determining criticality

In [SO05] we describe how to use the entanglement entropy and conformal field theory to determine the critical surfaces of a model. To this end, define the entropy of a block of  $\ell$  spins in a system of size  $N$  and inspired by the result (5.10) define the critical signature of the entropy,

$$s_\ell(c) = \frac{c}{3} \log_2 \sin \left( \frac{\pi \ell}{N} \right). \quad (5.37)$$

This signature should fit to the actual numerical values, subtracted the value at  $\ell = N/2$  since  $s_{1/2}(c) = 0$ . We define the error between the entropy data for a given model,  $\hat{s}_\ell$ , and the critical signature for a given central charge as

$$\varepsilon_c = \frac{1}{M} \sum_{\ell} (\hat{s}_\ell - s_\ell)^2. \quad (5.38)$$

Thus, the natural requirement is that this error is minimal. It is obvious that the error would be infinite if we included the endpoints in the error, since the critical signature diverges when  $\ell = 0$  or  $\ell = N$ , while the actual entropy would be zero in those cases (since the system is empty).

Moreover, we define an estimated central charge  $c_{\text{est}}$  as the central charge that minimizes this error,

$$c_{\text{est}} = \arg \min_c \left\{ \frac{1}{M} \sum_{\ell} (\hat{s}_\ell - s_\ell)^2 \right\} \quad (5.39)$$

where  $\hat{s}_\ell$  are the measured entanglement entropies.  $M$  is the number of lattice sites that are within the chosen cutoff. A convenient choice is to sum over values of  $\ell$  satisfying  $0.2N < \ell < 0.8N$ , and  $M$  follows subsequently.

It turns out that the error is very small also in near-critical systems, and a minimum in the error when adjusting parameters across a critical line not always corresponds very good to the actual phase transition. However, the if one looks at  $c_{\text{est}}$  when traversing a critical region, this almost always has a maximum at the critical point, except perhaps at confluence points<sup>5</sup>. Using the parameter value of that maximum and comparing to

---

<sup>5</sup>There are less well-defined critical regions, such as near the point  $\gamma = 0$ ,  $\lambda = 1$  in the XY model where two critical lines with different central charges intersect. Here the central charge is ill-defined, and the method inevitably fails. We denote these points in the parameter space confluence points.

the possible values of the central charge defined in (5.11), one can very often determine the central charge and critical parameter values with great certainty. The technique is illustrated for a critical line in the  $XYZ$  model in Figure 5.9.

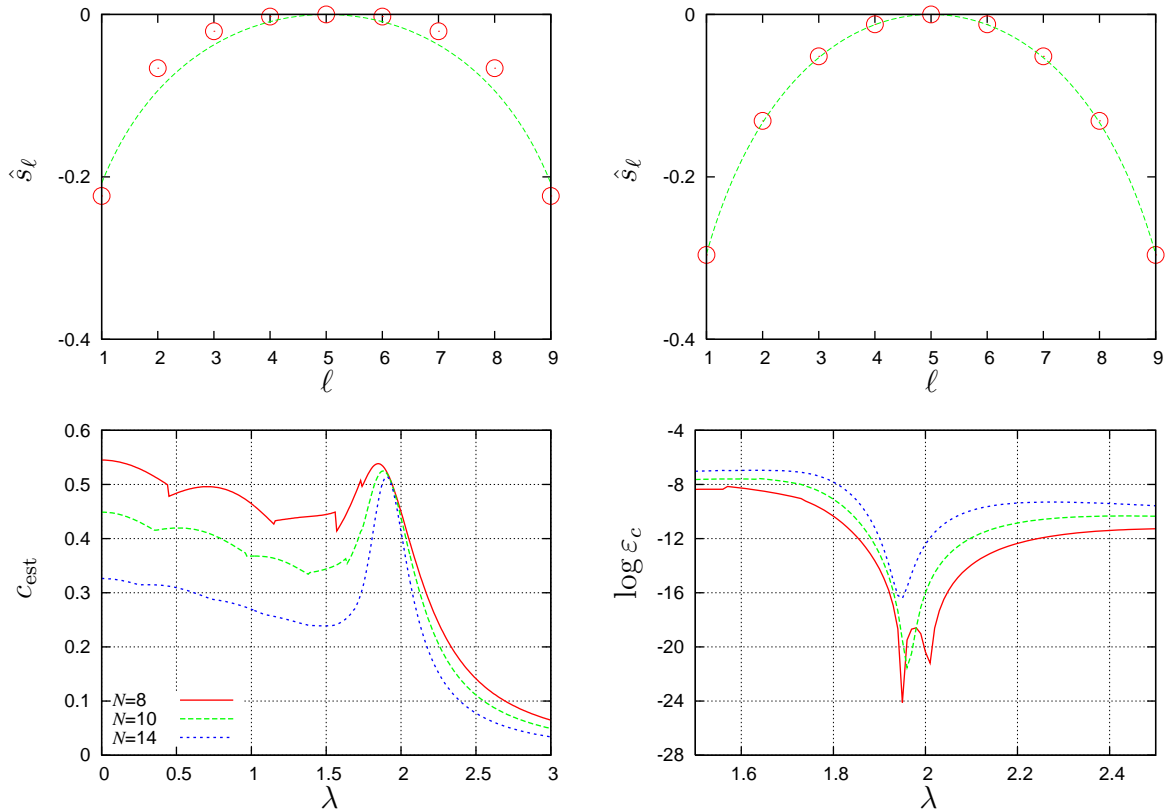


**Figure 5.9:** Illustration of the technique to find a critical line as described in the text. We traverse the parameter line in the  $XYZ$  model with  $\Delta = -1/2$ ,  $\gamma = 1$  and  $\lambda > 0$ . Top are  $\hat{s}_\ell$  and the critical entropy function (5.37) for off-critical ( $\lambda = 1$ , left with  $c_{\text{est}} \approx 0.368$ ) and near-critical ( $\lambda = 1.9$ , right with  $c_{\text{est}} \approx 0.512$ ) systems for  $N = 10$ . At bottom the estimated central charge and the error function (5.38) are shown when crossing the phase transition. We see the clear identification of the phase transition at  $\lambda_c = 1.9 \pm 0.05$ . The error function's minimum is at a slightly higher  $\lambda$  than the estimated central charge's maximum and the latter overshoots the assumed true value  $c = 0.5$  slightly. All this is in accordance with the benchmarking done in [SO05], and one may conclude that the critical point is at  $\lambda \approx 1.9$  with the Ising central charge  $c = 1/2$ .

## 5.5 Criticality in the $XYZ$ model

We extend the  $XY$  model into what we call the  $XYZ$  model, with Hamiltonian

$$H_{XYZ} = H_{XY} - \Delta \sum_n \sigma_n^z \sigma_{n+1}^z. \quad (5.40)$$

Despite the simple extension, this model cannot be fermionized in the way done with the  $XY$  model. Nevertheless, we can still find the critical regions and the corresponding central charges as described in Section 5.4.5 and Refs. [SO05, Skr05b]. When scanning a large portion of the parameter space, using  $N = 10$  (with symmetries) is useful, since the computation is rather reliable and the time consumption is reasonable. Near confluence points one can use larger systems for small areas of the space. All data in the next section are taken with  $N = 10$  to demonstrate the power of the method using such a small system.

### 5.5.1 Critical surfaces

We investigate the  $XYZ$  model in the range  $-2 < \Delta < 1/2$ ,  $\lambda > 0$ , and  $\gamma > 0$ . First, consider the case  $\gamma = 0$ , which is critical in the region shown in Figure 5.10. That is, in the region where  $\lambda < 1 - 2\Delta$  and  $\lambda$  larger than a lower limiting line as indicated in the figure.

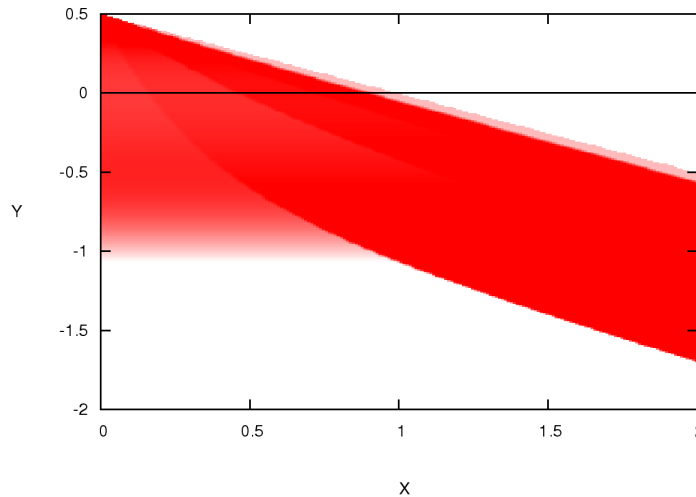


**Figure 5.10:** The critical region of the  $XYZ$  model with  $\gamma = 0$ . The critical surface has central charge  $c = 1$ , and is faded where the critical nature of the model becomes indeterminate for this determination which is done with  $N = 10$ . The black line indicates the intersection with the  $XY$  model. The model is symmetric under  $\lambda \rightarrow -\lambda$ .

In the region  $\Delta \approx -1$  and  $|\lambda| \lesssim 0.9$  the critical region ends in the sense that for smaller  $\Delta$  the model is massive, but the end of the criticality is indeterminate. This means that the estimated central charge falls below one, and the minimizing error gradually becomes larger, though there is no sharp transition to distinguish the critical from the non-critical region. The two lines mentioned above, however, have very sharp transitions between critical and non-critical regions and the central charge is readily identified at  $c = 1$ . The  $c = 1$  critical surface exclusively belongs to the regime  $\gamma = 0$ , except perhaps for  $\Delta < -1$ , where this surface seems to spread out into regions of non-zero  $\gamma$ . The details here are not investigated in detail, though.

In addition to the  $c = 1$  surface, there is a  $c = 1/2$  surface in the parameter space, which in the intersection with the  $XY$  model at  $\Delta = 0$  is at  $|\lambda| = 1$  for all  $\gamma$ s. When  $\Delta$  is larger than  $1/2$ , the  $c = 1$  critical surface vanishes for  $\gamma = 0$ , while the  $c = 1/2$ -line becomes indeterminate. However for  $\Delta < 1/2$ , the  $c = 1/2$  transition is illustrated in Figure 5.11. It has a very weak dependency on  $\gamma$ , and only for positive  $\Delta$ .

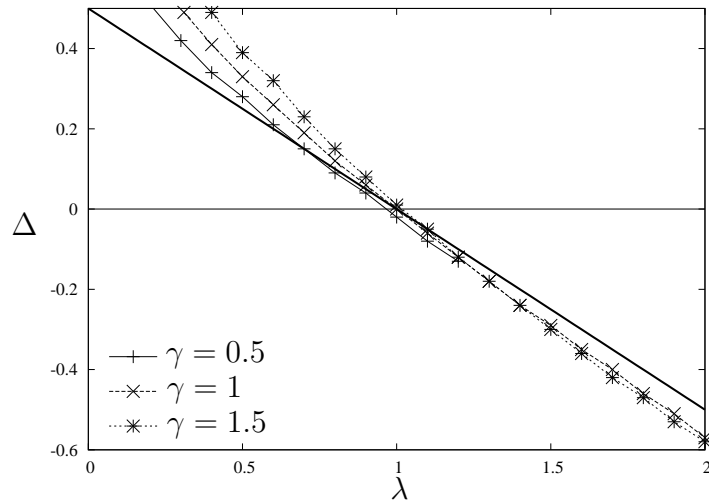


**Figure 5.11:** Intersections of the critical surface with  $c = 1/2$  in the  $XYZ$  model for three values of  $\gamma$  seen in the  $\Delta$ - $\lambda$  plane. There is an uncertainty in the  $\Delta$  value at each point of about  $\pm 10^{-2}$  due to the inherent uncertainty in the method. The lines are computed based on the maximal estimated central charge for  $N = 10$ . The horizontal line is the intersection with the  $XY$  model. Note that it is possible to draw the line for  $\gamma = 0.5$  only for  $\lambda < 1$ , since it becomes indeterminate for this system size for larger  $\lambda$ . This apparent indeterminacy is due to the proximity to the  $c = 1$  critical line, and larger system sizes will make it possible to draw this line further. The thick line is  $\lambda = 1 - 2\Delta$ , the end point of the  $c = 1$  surface, and presumed starting point for the  $c = 1/2$  surface for  $\gamma \rightarrow 0$ .

## 5.6 Time evolution

Given the formalism of the fermionization developed in section 5.4, it is easy to find the time evolution of the state [Skr06b]. In the Heisenberg picture, the Majorana fermions defined in (5.26) has a time evolution according to

$$\frac{d}{dt}\tilde{\gamma}_k = i[H, \tilde{\gamma}_k] = -2i \sum_i C_{ki} \tilde{\gamma}_i. \quad (5.41)$$

This is a linear first order system of differential equations, whose solution is

$$\tilde{\gamma}_k(t) = \mathbb{T}_{kl} \tilde{\gamma}_l, \quad (5.42)$$

where  $\tilde{\gamma}_k = \tilde{\gamma}_k(t=0)$ . The time evolution matrix  $\mathbb{T}$  is given by

$$\mathbb{T}_{kl}(t) = \sum_i S_{ki} S_{li}^* e^{-2i\xi_i t} \quad (5.43)$$

when  $S$  is the eigenvector matrix of  $\mathcal{C}$  and  $\xi$  are the eigenvalues.

A state that is in a thermal equilibrium with its environment at an inverse temperature  $\beta$  is a mixed state described by its density matrix,

$$\sigma = \frac{1}{\mathcal{Z}} e^{-\beta H} \quad (5.44)$$

where  $H$  is the system's Hamiltonian and  $\mathcal{Z} = \text{Tr} e^{-\beta H}$  is the partition function. Given a basis in which the Hamiltonian is diagonal  $H = \sum_k E_k |\psi_k\rangle\langle\psi_k|$ , this becomes

$$\sigma = \frac{1}{\mathcal{Z}} \sum_k e^{-\beta E_k} |\psi_k\rangle\langle\psi_k|.$$

In [Skr06b] we compute the time evolution of an excited pure state in an Ising chain with a magnetic impurity, and show that the eigenvalues of the reduced density matrix for a part of the chain resembles those for a state in thermal equilibrium at some temperature  $\beta^{-1}$ . To this end, we compute the classical fidelity between the eigenvalues. If we denote the ordered eigenvalues of the reduced density matrix  $\lambda_k$  and the thermal density matrix  $\varphi_k = e^{-\beta E_k} / \mathcal{Z}$ , the classical fidelity becomes

$$F_c(\lambda, \varphi) = \sum_n \sqrt{\lambda_n \varphi_n}.$$

The classical fidelity is an adequate measure of the distance between two probability distributions, being 1 if the distributions are equal, and less than one else. Hence the fidelity is not a metric, but is intimately related to the trace distance, which is, and thus can be considered equivalent to a metric [NC00].

For two arbitrary quantum states described by density matrices  $\rho$  and  $\sigma$ , the fidelity between them is defined as

$$F(\rho, \sigma) = \text{Tr} \sqrt{\rho^{1/2} \sigma \rho^{1/2}}, \quad (5.45)$$

which reduces to the classical fidelity of their eigenvalues in the case where  $\rho$  and  $\sigma$  commute. However, for the non-commuting case, it gets more complicated. Given that the two states can be fermionized, and thus written in terms of the Majorana fermions

$$\begin{aligned} \rho &= N_\rho \exp \left( - \sum_{kl} \Omega_{kl} \check{\gamma}_k \check{\gamma}_l \right) & N_\rho &= \frac{1}{\prod_k (1 + e^{-\Omega_{kk}})} \\ \sigma &= N_\sigma \exp \left( - \sum_{kl} \beta E_{kl} \check{\gamma}_k \check{\gamma}_l \right) & N_\sigma &= \frac{1}{\prod_k (1 + e^{-\beta E_{kk}})}, \end{aligned}$$

we need to compute the matrix product  $\sigma^{1/2} \rho \sigma^{1/2}$ . The Campbell-Baker-Hausdorff formula for exponentials of non-commuting variables  $\mathcal{A}$  and  $\mathcal{B}$  reads

$$\begin{aligned} e^{\mathcal{A}} e^{\mathcal{B}} &= e^{\mathcal{D}} \quad \text{where} \\ \mathcal{D} &= \mathcal{A} + \mathcal{B} + \frac{1}{2} [\mathcal{A}, \mathcal{B}] + \frac{1}{12} [\mathcal{A} - \mathcal{B}, [\mathcal{A}, \mathcal{B}]] + \dots, \end{aligned} \quad (5.46)$$

given that the series converges (which is not obvious). If we have operators  $\Theta = \frac{1}{2} \theta_{ij} \check{\gamma}_i \check{\gamma}_j$  and  $\Xi = \frac{1}{2} \xi_{ij} \check{\gamma}_i \check{\gamma}_j$  for some anti-symmetric matrices  $\theta$  and  $\xi$ , we can use the commutator-anti-commutator relation

$$\begin{aligned} [\check{\gamma}_i \check{\gamma}_j, \check{\gamma}_i \check{\gamma}_j] &= \check{\gamma}_i \{ \check{\gamma}_j, \check{\gamma}_k \} \check{\gamma}_l - \check{\gamma}_i \check{\gamma}_k \{ \check{\gamma}_j, \check{\gamma}_l \} + \{ \check{\gamma}_i, \check{\gamma}_k \} \check{\gamma}_l \check{\gamma}_j - \check{\gamma}_k \{ \check{\gamma}_i, \check{\gamma}_l \} \check{\gamma}_j \\ &= \delta_{jk} \check{\gamma}_i \check{\gamma}_l - \delta_{jl} \check{\gamma}_i \check{\gamma}_k + \delta_{ik} \check{\gamma}_l \check{\gamma}_j - \delta_{il} \check{\gamma}_k \check{\gamma}_j \end{aligned}$$

to find that

$$[\Theta, \Xi] = \frac{1}{2} \varphi_{ij} \check{\gamma}_i \check{\gamma}_j = \Phi \quad (5.47)$$

where  $\varphi = [\theta, \xi]$ . This relation holds for all iterated commutators involved in (5.46), and we may therefore conclude that

$$e^{\mathcal{A}} e^{\mathcal{B}} = e^{\mathcal{D}},$$

where  $\mathcal{A} = \frac{1}{2} A_{ij} \check{\gamma}_i \check{\gamma}_j$ ,  $\mathcal{B} = \frac{1}{2} B_{ij} \check{\gamma}_i \check{\gamma}_j$ , and  $\mathcal{D} = \frac{1}{2} D_{ij} \check{\gamma}_i \check{\gamma}_j$  with  $D$  given by the expansion (5.46). The generalization to more than two factors is simple, and we can compute the matrix product  $\sigma^{1/2} \rho \sigma^{1/2}$  and (block) diagonalize the result into the matrix  $\exp(-K_{ij} \hat{\gamma}_i \hat{\gamma}_j)$  with new Majorana fermions  $\hat{\gamma}$ . Thus the fidelity becomes

$$F(\sigma, \rho) = \text{Tr} \sqrt{N_\sigma N_\rho} e^{-\frac{1}{2} K_{ij} \hat{\gamma}_i \hat{\gamma}_j},$$

which is straightforward to compute.

Hence it is possible to find the full fidelity rather than just the classical fidelity of the eigenvalues, with the possible catch that the Campbell-Baker-Hausdorff series (5.46) may

not converge. However, it is not expected that the difference between the classical and quantum versions will be large, since the diagonalization of the Hamiltonian and the density matrix will be “almost” the same. That is, the diagonalization matrices  $O_\sigma$  and  $O_\rho$  respectively fulfill  $O_\sigma^{-1}O_\rho \approx \mathbb{1}$ . However, discrepancies in this equality may map back to small eigenvalues that are of little importance to the fidelity.

## 5.7 The quantum Hall effects

The exposure of an essentially two dimensional conductor to an magnetic field gives rise to a voltage perpendicular to the current flowing through the slab, which has long been recognized as the Hall effect. A schematic experimental setup is shown in Figure 5.12. The Hall resistance  $R_{xy}$  is the Hall voltage across the slab  $V_y$  by the exposed current  $I_x$ , and in the classical case the Hall voltage is proportional to the imposed magnetic field. Indeed, straightforward calculation gives the law  $R_{xy} = B/ne$ ,  $B$  being the perpendicular magnetic

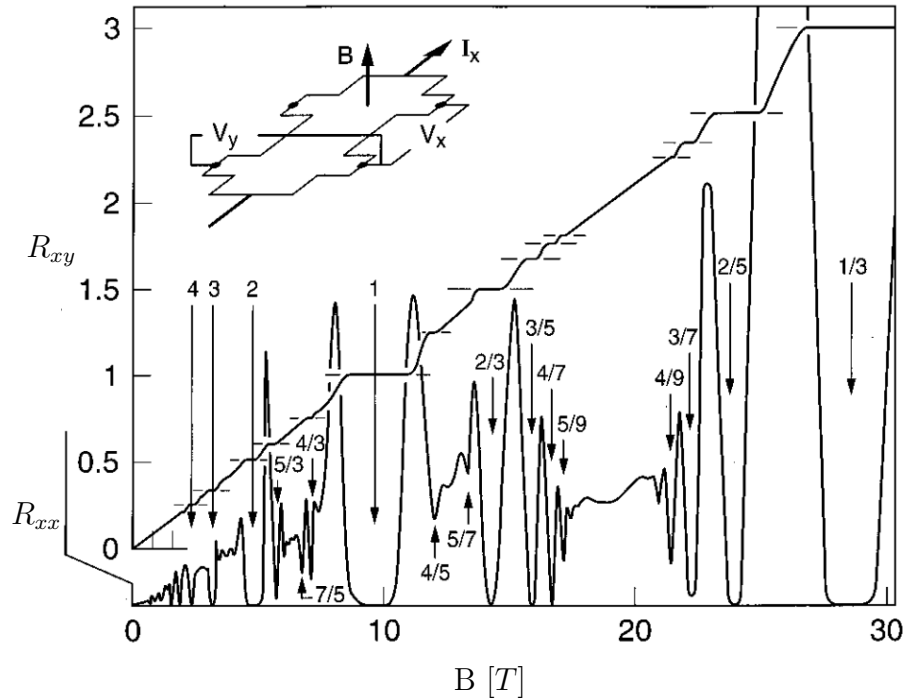


**Figure 5.12:** The resistivity of a quantum Hall system, sketched in the upper left. Both resistivities in orthogonal  $R_{xx} = V_x/I_x$  and transverse  $R_{xy} = V_y/I_x$  are shown and the most important fractional and integer quantum Hall states are indicated. The experiment uses a 2D system with electron density  $n = 2.33 \times 10^{15} \text{m}^{-2}$  cooled to 85mK. Image from [STG99].

field,  $n$  the density of conduction electrons<sup>6</sup> and  $e$  the elementary charge. When the system is cooled down, and the magnetic field becomes large, the Hall resistance becomes quantized at exact levels of

$$\nu = \frac{N_e h}{eB} = \frac{N_e}{N_s}; \quad N_s = \frac{eB}{h},$$

with  $\nu$  an integer called the filling factor, as first reported in 1980 by von Klitzing *et al.* [KDP80].  $h$  is Planck's constant, and the phrase *filling factor* refers to the fact that  $N_s$  is the number of available states in each Landau level and  $N_e$  the number of available electrons. As the magnetic field is increased,  $N_s$  increases proportionally, and when  $\nu$  becomes integer, the Fermi level resides between Landau levels, thus all available states are occupied and the electron fluid is essentially incompressible until the magnetic field increases to another integer. This integer quantum Hall effect (IQHE) is explained as a problem of non-interacting (apart from the Fermi statistics) electron problem first explained by Laughlin in 1981 [Lau81].

In 1982 Tsui *et al.* [TSG82] identified levels of constant resistance also at levels of fractional  $\nu$ , a result completely unexpected at the time, and a matter much harder to explain than IQHE. The fractional quantum Hall effect (FQHE) occurs at filling factors  $\nu = p/q$  for certain fractions, where the most prominent levels are those with  $\nu = 1/q$  and  $\nu = 1 - 1/q$  with  $q$  odd (called primary states), and  $\nu = p/(2p \pm 1)$  (higher order states), cf. Figure 5.12. However, many more fractions appear, even fractions with even denominator. FQHE is, in contrast to the integer variant a complex many-particle problem, and a number of explanations exist. Perhaps the most prominent of these are Laughlin's trial wave function [Lau83], which for the  $\nu = 1/q$  state of  $n$  particles reads

$$\psi_{1/q}(z_1, \dots, z_n) = \prod_{i < j} (z_i - z_j)^q \exp\left(-\frac{1}{4l_0^2} \sum_{k=1}^n |z_k|^2\right),$$

where  $z_k$  is the 2D complex position of particle  $k$ , and normalization is omitted.  $l_0 = \sqrt{\hbar/eB}$  is the magnetic length. This reflects attaching  $q$  flux quanta to each electron, since the charge concentration of electrons and charge deficit of a vortex associated with a flux quantum attract each other, thus creating fractionally charged excitations.

More recently, Jain's composite fermion picture [Jai89] has become a more fashionable explanation, particularly since it also explains many higher-order states. Essentially, the system of strongly interacting electrons in a strong magnetic field is mapped onto a system with a reduced magnetic field and a series of non-interacting composite fermions consisting of one electron and two flux quanta [Jai00]. Thus, the fractional quantum Hall effect becomes an integer quantum Hall problem of fractionally charged fermions.

---

<sup>6</sup>In a typical setup one uses GaAs/AlGaAs heterostructures with  $n \sim 10^{15} \text{m}^{-2}$ . [STG99]



### 5.7.1 FQHE on a torus

Most of the literature has so far focused on explaining the inner workings of the FQHE, and little is known about the entanglement properties of the quantum Hall states. Nevertheless, it has been argued that on the IQHE plateaus the entanglement is zero, since this is essentially a non-interacting system [Shi04]. As the magnetic field is increased (or decreased) and the plateau changes from one FQHE state to another, we have a quantum phase transition, and possibly the criticality technique described in [SO05] and Section 5.4.5 could be applied here.

Even though the QHE system is a generic two dimensional problem, it can be mapped onto a 1D problem [CP95, YHL83]. That is, with periodic boundary conditions, one have  $N$  different single-particle wave functions in each Landau level, which in a rectangular geometry with sides  $L_x$  and  $L_y$  are

$$\psi_j(\mathbf{r}) = \left( \frac{1}{L_y \sqrt{\pi l_0}} \right)^{1/2} \sum_{k=-\infty}^{\infty} \exp \left[ \frac{i}{l_0^2} (X_j + kL_x)y - \frac{1}{2l_0^2} (X_j + kL_x - x)^2 \right]. \quad (5.48)$$

Here,  $1 \leq j \leq N_s$  and  $X_j = jL_x/N_s$  are localizations along the  $x$ -direction<sup>7</sup>. This amounts to  $N_s$  localizations along the  $x$  direction with Gaussian with of the order of the magnetic length. The probability distribution is independent of  $y$ .

In a second quantized version, the Hamiltonian is

$$H = \sum_j \mathcal{W} a_j^\dagger a_j + \sum_{j_1} \sum_{j_2} \sum_{j_3} \sum_{j_4} \mathcal{A}_{j_1, j_2, j_3, j_4} a_{j_1}^\dagger a_{j_2}^\dagger a_{j_3} a_{j_4} \quad (5.49)$$

where  $a_j$  is the destruction operator at site  $j$ . The single electron energy  $\mathcal{W}$  is a known constant [YHL83] and the coupling term is

$$\begin{aligned} \mathcal{A}_{j_1, j_2, j_3, j_4} &= \frac{1}{2} \int d^2 \mathbf{r}_1 d^2 \mathbf{r}_2 \psi_{j_1}^*(\mathbf{r}_1) \psi_{j_2}^*(\mathbf{r}_2) V(\mathbf{r}_1 - \mathbf{r}_2) \psi_{j_3}(\mathbf{r}_2) \psi_{j_4}(\mathbf{r}_1) \\ &= \frac{\pi e^2}{\varepsilon_0 L_x L_y} \sum_{\mathbf{q} \neq 0} \frac{1}{q} \exp \left[ -\frac{1}{2} l_0^2 q^2 - i q_x L_x (j_1 - j_3) / N_s \right] \delta'_{j_1 - j_4, q_y L_y / 2\pi} \delta'_{j_1 + j_2, j_3 + j_4} \end{aligned}$$

where  $\delta'$  is a Kronecker delta modulus  $N_s$  and  $V(\mathbf{r})$  is the real-space Coulomb interaction. The sum over  $\mathbf{q}$  is a sum over all allowed  $\mathbf{q}$ -vectors (except the zero vector), that is with integers  $s$  and  $t$  such that  $\mathbf{q} = \left( \frac{2\pi s}{L_x}, \frac{2\pi t}{L_y} \right)$ . Thus a basis of the Hilbert space is defined by the  $N_e$  occupation numbers,  $|j_1, \dots, j_{N_e}\rangle$ . For a given filling fraction  $\nu$  this means that the Hilbert space has dimension  $\binom{N_s}{N_e}$ , which obviously quickly becomes far too large to handle. Indeed, the Hilbert space's dimension grows exponentially with the number of electrons for a fixed  $\nu$ , and faster than  $2^{N_e}$ . Again, utilizing symmetries makes it possible to go slightly

<sup>7</sup>This example is in the Landau gauge  $\mathbf{A} = Bx\hat{y}$ .

further. With the most naïve approach however, investigating six particles in a  $\nu = 1/3$  system involves matrices of size  $\binom{18}{6} = 18564$ , which is computationally time consuming. Larger systems are essentially inaccessible.

### 5.7.2 Entanglement in the FQHE

The entanglement in the FQHE case is conceptually different from the spin chains setting. This is mainly due to the complications involved in dealing with identical particles. In spin chains we consider each particle fixed with a non-overlapping wave function, and the particles can hence be thought of as separate, or non-identical. This is not the case in the FQHE where the overlap of the wave function may be considerable. Entanglement is ill-defined in this case, mainly since the anti-symmetrized wave function defined by the Slater determinant already carries quantum correlations while the particles involved cannot be said to be entangled, in the sense that there exists no less correlated state. It has been suggested that entropy of reduced density matrices larger than that of a Slater determinant state is an entangled fermion state [GM04]. For bosons the argument is likewise, but since the least correlated bosonic state is a product state whose entropy is zero, positive entropy indicates an entangled state here. However, it is not obvious that the entropy (possibly subtracted the Slater determinant entropy) is a genuine entanglement measure. The entropy of a single particle in a Slater determinant with  $N$  particles is  $\log_2 N$ .

For the FQHE case the reduced density matrix of  $N'_e < N_e$  electrons is of size  $\binom{N_s}{N'_e}$  and thus the reduced density matrix may be *larger* than the original matrix, if  $N'_e > N_e/2$ . Despite this apparent paradox, it is possible to compute the entropy of the reduced density matrix. To this end, consider the density matrix of the  $\binom{3}{2}$  system in the basis  $\{|110\rangle, |101\rangle, |011\rangle\}$ ,  $\rho = [\rho_{ij}]$  in this basis. Tracing out one particle to remain with one amounts to tracing over all wave functions with one particle, and in the new basis  $\{|100\rangle, |010\rangle, |001\rangle\}$  this becomes

$$\rho' = \langle 1 \cdot \cdot | \rho | 1 \cdot \cdot \rangle + \langle \cdot 1 \cdot | \rho | \cdot 1 \cdot \rangle + \langle \cdot \cdot 1 | \rho | \cdot \cdot 1 \rangle = \frac{1}{2} \begin{bmatrix} \rho_{11} + \rho_{22} & \rho_{23} & \rho_{13} \\ \rho_{32} & \rho_{11} + \rho_{33} & \rho_{12} \\ \rho_{31} & \rho_{21} & \rho_{22} + \rho_{33} \end{bmatrix}.$$

Numerical calculation of the entropy for the ground state of (5.49) by the prescription above, shows that the integer quantum Hall effect has entropy  $S_n = \log_2 \binom{N_s}{n}$  when the system is traced out to leave  $n$  particles, as predicted in [ILO06]. Tracing out to a single particle, the entropy is simply  $S_1 = \log_2 N_e$ . The values for the entropy in the IQHE states are independent of the nature of the interaction, since IQHE is an essentially non-interacting phenomenon.

For the FQHE the case is more complicated, and exact analytical results are rare. Using the prescription above, some basic results for very few particles can be found. In particular, we find that in the limit where  $L_y \ll L_x$ , the entropy is exactly that of the IQHE,  $\log_2 \binom{N_s}{n}$

when  $n$  particles are traced out. In this limit, the localizations are so far apart that the particles are essentially non-interacting, and the IQHE regime is recovered. However, as the aspect ratio  $L_y/L_x$  is increased, at some value the entropy for a single particle jumps discontinuously to a higher value, and after this increases slowly with the aspect ratio until saturating.



# Bibliography

- [ABV01] M. C. ARNESEN, S. BOSE, AND V. VEDRAL, *Natural Thermal and Magnetic Entanglement in the 1D Heisenberg Model*, Phys. Rev. Lett., **87**, 017901 (2001).
- [ADD<sup>+</sup>06] A. ANDRÉ, D. DEMILLE, J. M. DOYLE, M. D. LUKIN, S. E. MAXWELL, P. RABL, R. J. SCHOELKOPF, AND P. ZOLLER, *A coherent all-electrical interface between polar molecules and mesoscopic superconducting resonators*, Nature Phys., **2**, 636 (2006).
- [ADR82] A. ASPECT, J. DALIBARD, AND G. ROGER, *Experimental Test of Bell's Inequalities Using Time-Varying Analyzers*, Phys. Rev. Lett., **49**, 1804 (1982).
- [BB84] C. H. BENNETT AND G. BRASSARD, *Quantum cryptography: Public key distribution and coin tossing*, in *Proceedings of the IEEE International Conference on Computers, Systems and Signal Processing, Bangalore, India*, p. 175 (IEEE Press, New York, 1984).
- [BBC<sup>+</sup>93] C. H. BENNETT, G. BRASSARD, C. CRÉPEAU, R. JOZSA, A. PERES, AND W. K. WOOTTERS, *Teleporting an unknown quantum state via dual classical and Einstein-Podolsky-Rosen channels*, Phys. Rev. Lett., **70**, 1895 (1993).
- [Bel64] J. S. BELL, *On the Einstein Podolsky Rosen Paradox*, Physics, **1**, 195 (1964).
- [BM71] E. BAROUCH AND B. M. MCCOY, *Statistical Mechanics of the XY model. II. Spin-Correlation Functions*, Phys. Rev. A, **3**, 786 (1971).
- [BPZ84] A. A. BELAVIN, A. M. POLYAKOV, AND A. B. ZAMOLODCHIKOV, *Infinite conformal symmetry in two-dimensional quantum field theory*, Nucl. Phys. B, **241**, 333 (1984).
- [BW92] C. H. BENNETT AND S. J. WIESNER, *Communication via one- and two-particle operators on Einstein-Podolsky-Rosen states*, Phys. Rev. Lett., **69**, 2881 (1992).
- [CC04] P. CALABRESE AND J. CARDY, *Entanglement Entropy and Quantum Field Theory*, J. Stat. Mech., p. P06002 (2004).

- [CC05] ———, *Evolution of Entanglement Entropy in One-Dimensional Systems*, J. Stat. Mech., p. P04010 (2005).
- [Cha02] S. CHAKRAVARTY, *Theory of the  $d$ -density wave from a vertex model and its implications*, Phys. Rev. B, **66**, 224505 (2002).
- [Chr06] M. CHRISTANDL, *The Structure of Bipartite Quantum States - Insights from Group Theory and Cryptography*, Ph.D. thesis, University of Cambridge (2006), [quant-ph/0604183].
- [CP95] T. CHAKRABORTY AND P. PIETILÄINEN, *The Quantum Hall Effects: Fractional and Integral* (Springer, Berlin, 1995).
- [CW94] C. CALLAN AND F. WILCZEK, *On Geometric Entropy*, Phys. Lett. B, **333**, 55 (1994).
- [CW04] M. CHRISTANDL AND A. WINTER, *“Squashed Entanglement” - An Additive Entanglement Measure*, J. Math. Phys., **45**, 829 (2004).
- [CZ95] J. I. CIRAC AND P. ZOLLER, *Quantum Computations with Cold Trapped Ions*, Phys. Rev. Lett., **74**, 4091 (1995).
- [EC05] J. EISERT AND M. CRAMER, *Single-copy entanglement in critical quantum spin chains*, Phys. Rev. A, **72**, 042112 (2005).
- [Eke91] A. K. EKERT, *Quantum cryptography based on Bell’s theorem*, Phys. Rev. Lett., **67**, 661 (1991).
- [EPR35] A. EINSTEIN, B. PODOLSKY, AND N. ROSEN, *Can Quantum-Mechanical Description of Physical Reality Be Considered Complete?*, Phys. Rev., **47**, 777 (1935).
- [Fey82] R. P. FEYNMAN, *Simulating Physics with Computers*, Int. J. Theor. Phys., **21**, 467 (1982).
- [FMS97] P. D. FRANCESCO, P. MATHIEU, AND D. SÉNÉCHAL, *Conformal Field Theory* (Springer, New York, 1997).
- [FQS84] D. FRIEDAN, Z. QIU, AND S. SHENKER, *Conformal Invariance, Unitarity, and Critical Exponents in Two Dimensions*, Phys. Rev. Lett., **52**, 1575 (1984).
- [Gin89] P. GINSPARG, *Applied conformal field theory*, in E. BRÉZIN AND J. Z. JUSTIN (editors), *Fields, Strings and Critical Phenomena* (Les Houches, Session XLIX, 1989).

- 
- [GKLC01] G. GIEDKE, B. KRAUS, M. LEWENSTEIN, AND J. I. CIRAC, *Entanglement Criteria for all Bipartite Gaussian States*, Phys. Rev. Lett., **87**, 167904 (2001).
- [GM04] G. GHIRARDI AND L. MARINATTO, *General criterion for the entanglement of two indistinguishable particles*, Phys. Rev. A, **70**, 012109 (2004).
- [GWK<sup>+</sup>03] G. GIEDKE, M. M. WOLF, O. KRÜGER, R. F. WERNER, AND J. I. CIRAC, *Entanglement of Formation for Symmetric Gaussian States*, Phys. Rev. Lett., **91**, 107901 (2003).
- [Haw75] S. HAWKING, *Comm. Math. Phys.*, **43**, 199 (1975).
- [HHH00] M. HORODECKI, P. HORODECKI, AND R. HORODECKI, *Limits for Entanglement Measures*, Phys. Rev. Lett., **84**, 2014 (2000).
- [HLW94] C. HOLZHEY, F. LARSEN, AND F. WILCZEK, *Geometric and Renormalized Entropy in Conformal Field Theory*, Nucl.Phys. B, **424**, 443 (1994).
- [HW97] S. HILL AND W. K. WOOTTERS, *Entanglement of a Pair of Quantum Bits*, Phys. Rev. Lett., **78**, 5022 (1997).
- [ILO06] S. IBLISDIR, J. I. LATORRE, AND R. ORÚS, *Entropy and Exact Matrix Product Representation of the Laughlin Wave Function* (2006), [cond-mat/0609088].
- [Jai89] J. K. JAIN, *Composite-fermion approach for the fractional quantum Hall effect*, Phys. Rev. Lett., **63**, 199 (1989).
- [Jai00] ———, *The composite fermion: A quantum particle and its quantum fluids*, Physics Today, **53**, 39 (2000).
- [Jen05] R. JENSSEN, *An Information Theoretic Approach to Machine Learning*, Ph.D. thesis, The University of Tromsø, Norway (2005).
- [Kad66] L. P. KADANOFF, *Scaling laws for Ising models near  $T_c$* , Physics, **2**, 263 (1966).
- [KDP80] K. V. KLITZING, G. DORDA, AND M. PEPPER, *New Method for High-Accuracy Determination of the Fine-Structure Constant Based on Quantized Hall Resistance*, Phys. Rev. Lett., **45**, 494 (1980).
- [KE04] H. J. KIMBLE AND S. J. VAN ENK, *Push-button teleportation*, Nature, **429**, 712 (2004).
- [Kor04] V. E. KOREPIN, *Universality of Entropy Scaling in One Dimensional Gapless Models*, Phys. Rev. Lett., **92**, 096402 (2004).

- [KT73] J. M. KOSTERLITZ AND D. J. THOULESS, *Ordering, metastability and phase transitions in two-dimensional systems*, Journal of Physics C: Solid State Physics, **6**, 1181 (1973).
- [Lau81] R. B. LAUGHLIN, *Quantized Hall conductivity in two dimensions*, Phys. Rev. B, **23**, 5632 (1981).
- [Lau83] ———, *Anomalous Quantum Hall Effect: An Incompressible Quantum Fluid with Fractionally Charged Excitations*, Phys. Rev. Lett., **50**, 1395 (1983).
- [Lie67] E. H. LIEB, *Residual Entropy of Square Ice*, Phys. Rev., **162**, 162 (1967).
- [Llo99] S. LLOYD, *Quantum search without entanglement*, Phys. Rev. A, **61**, 010301 (1999).
- [LLRV05] J. I. LATORRE, C. A. LÜTKEN, E. RICO, AND G. VIDAL, *Fine-grained entanglement loss along renormalization-group flows*, Phys. Rev. A, **71**, 034301 (2005).
- [LRV04] J. I. LATORRE, E. RICO, AND G. VIDAL, *Ground state entanglement in quantum spin chains*, Quant. Inf. and Comp., **4**, 48 (2004), [quant-ph/0304098].
- [Mer85] N. D. MERMIN, *Is the moon there when nobody looks? Reality and the quantum theory*, Physics Today, **38**, 38 (1985).
- [MW66] N. D. MERMIN AND H. WAGNER, *Absence of Ferromagnetism or Antiferromagnetism in One- or Two-Dimensional Isotropic Heisenberg Models*, Phys. Rev. Lett., **17**, 1133 (1966).
- [Myh04] G. O. MYHR, *Measures of entanglement in quantum mechanics*, Master's thesis, NTNU, Norway (2004), [quant-ph/0408094].
- [NC00] M. A. NIELSEN AND I. L. CHUANG, *Quantum Computation and Quantum Information* (Cambridge University Press, Cambridge, UK, 2000).
- [OAFF02] A. OSTERLOH, L. AMICO, G. FALCI, AND R. FAZIO, *Scaling of entanglement close to a quantum phase transition*, Nature, **416**, 608 (2002).
- [ON02a] T. J. OSBORNE AND M. A. NIELSEN, *Entanglement in simple quantum phase transitions*, Phys. Rev. A, **66**, 032110 (2002).
- [ON02b] ———, *Entanglement, Quantum Phase Transitions, and Density Matrix Renormalization*, Quant. Inf. Proc., **1**, 45 (2002).
- [Ons44] L. ONSAGER, *Crystal Statistics. I. A Two-Dimensional Model with an Order-Disorder Transition*, Phys. Rev., **65**, 117 (1944).



- 
- [Ort05] E. R. ORTEGA, *Quantum correlations in (1+1)-dimensional systems*, Ph.D. thesis, Universitat de Barcelona, Spain (2005), [quant-ph/0509037].
- [Pol70] A. M. POLYAKOV, *Conformal symmetry of critical fluctuations*, JETP Lett., **12**, 381 (1970).
- [SAB<sup>+</sup>06] M. STEFFEN, M. ANSMANN, R. C. BIALCZAK, N. KATZ, E. LUCERO, R. McDERMOTT, M. NEELEY, E. M. WEIG, A. N. CLELAND, AND J. M. MARTINIS, *Measurement of the Entanglement of Two Superconducting Qubits via State Tomography*, Science, **313**, 1423 (2006).
- [Sac99] S. SACHDEV, *Quantum Phase Transitions* (Cambridge University Press, Cambridge, UK, 1999).
- [SC06] O. F. SYLJUÅSEN AND S. CHAKRAVARTY, *Resonating Plaquette Phase of a Quantum Six-Vertex Model*, Phys. Rev. Lett., **96**, 147004 (2006).
- [Sch05] U. SCHOLLWÖCK, *The density-matrix renormalization group*, Rev. Mod. Phys., **77**, 259 (2005).
- [Shi04] Y. SHI, *Quantum entanglement in second-quantized condensed matter systems*, J. Phys. A, **37**, 6807 (2004).
- [Sho94] P. SHOR, *Algorithms for Quantum Computation: Discrete Logarithms and Factoring*, in S. GOLDWASSER (editor), *Proceedings of the 35<sup>th</sup> Annual Symposium on Foundations of Computer Science*, p. 124 (IEEE Press, Los Alamitos, California, 1994).
- [Skr05a] S. O. SKRØVSETH, *Entanglement in bosonic systems*, Phys. Rev. A, **72**, 062305 (2005).
- [Skr05b] ———, *Entanglement signatures in critical quantum systems*, in *ERATO conference on Quantum Information Science*, p. 177 (Quantum Computation and Information Project, ERATO, JST, Tokyo, Japan, 2005).
- [Skr06a] ———, *Entanglement properties of quantum spin chains*, Phys. Rev. A, **74**, 022327 (2006).
- [Skr06b] ———, *Thermalization through unitary evolution of pure states*, Europhys. Lett., **76**, 1179 (2006).
- [Sla41] J. C. SLATER, *Theory of the Transition in KH<sub>2</sub>PO<sub>4</sub>*, J. Chem. Phys., **9**, 16 (1941).
- [SO05] S. O. SKRØVSETH AND K. OLAUSSEN, *Entanglement used to identify critical systems*, Phys. Rev. A, **72**, 022318 (2005).

- [Sre93] M. SREDNICKI, *Entropy and Area*, Phys. Rev. Lett., **71**, 666 (1993).
- [STG99] H. L. STORMER, D. C. TSUI, AND A. C. GOSSARD, *The fractional quantum Hall effect*, Rev. Mod. Phys., **71**, S298 (1999).
- [Sut70] B. SUTHERLAND, *Two-Dimensional Hydrogen Bonded Crystals without the Ice Rule*, J. Math. Phys., **11**, 3183 (1970).
- [TSG82] D. C. TSUI, H. L. STORMER, AND A. C. GOSSARD, *Two-Dimensional Magnetotransport in the Extreme Quantum Limit*, Phys. Rev. Lett., **48**, 1559 (1982).
- [VC04] F. VERSTRAETE AND J. I. CIRAC, *Renormalization algorithms for Quantum-Many Body Systems in two and higher dimensions* (2004), [cond-mat/0407066].
- [Vid03] G. VIDAL, *Efficient Classical Simulation of Slightly Entangled Quantum Computations*, Phys. Rev. Lett., **91**, 147902 (2003).
- [Vid05] ———, *Entanglement renormalization* (2005), [cond-mat/0512165].
- [VLRK02] G. VIDAL, J. I. LATORRE, E. RICO, AND A. KITAEV, *Entanglement in quantum critical phenomena*, Phys. Rev. Lett., **90**, 227902 (2002).
- [VPRK97] V. VEDRAL, M. B. PLENIO, M. A. RIPPIN, AND P. L. KNIGHT, *Quantifying Entanglement*, Phys. Rev. Lett., **78**, 2275 (1997).
- [VSB<sup>+</sup>01] L. M. K. VANDERSYPEN, M. STEFFEN, G. BREYTA, C. S. YANNONI, M. H. SHERWOOD, AND I. L. CHUANG, *Experimental realization of Shor's quantum factoring algorithm using nuclear magnetic resonance*, Nature, **414**, 883 (2001).
- [VW02] G. VIDAL AND R. F. WERNER, *Computable measure of entanglement*, Phys. Rev. A, **65**, 032314 (2002).
- [VWPGC06] F. VERSTRAETE, M. M. WOLF, D. PEREZ-GARCIA, AND J. I. CIRAC, *Criticality, the Area Law, and the Computational Power of Projected Entangled Pair States*, Phys. Rev. Lett., **96**, 220601 (2006).
- [Wan01a] X. WANG, *Effects of anisotropy on thermal entanglement*, Phys. Lett. A, **281**, 101 (2001).
- [Wan01b] ———, *Entanglement in the quantum Heisenberg XY model*, Phys. Rev. A, **64**, 012313 (2001).
- [WDM<sup>+</sup>05] T.-C. WEI, D. DAS, S. MUKHOPADYAY, S. VISHVESHWARA, AND P. M. GOLDBART, *Global entanglement and quantum criticality in spin chains*, Phys. Rev. A, **71**, 060305(R) (2005).

- 
- [Wer89] R. F. WERNER, *Quantum states with Einstein-Podolsky-Rosen correlations admitting a hidden-variable model*, Phys. Rev. A, **40**, 4277 (1989).
- [WKG<sup>+</sup>04] M. M. WOLF, G. GIEDKE, O. KRÜGER, R. F. WERNER, AND J. I. CIRAC, *Gaussian entanglement of formation*, Phys. Rev. A, **69**, 052320 (2004).
- [Whi92] S. R. WHITE, *Density matrix formulation for quantum renormalization groups*, Phys. Rev. Lett., **69**, 2863 (1992).
- [Wil75] K. G. WILSON, *The renormalization group: critical phenomena and the Kondo problem*, Rev. Mod. Phys., **47**, 773 (1975).
- [WN92] S. R. WHITE AND R. M. NOACK, *Real-space quantum renormalization groups*, Phys. Rev. Lett., **68**, 3487 (1992).
- [Woo98] W. K. WOOTTERS, *Entanglement of Formation of an Arbitrary State of Two Qubits*, Phys. Rev. Lett., **80**, 2245 (1998).
- [YHL83] D. YOSHIOKA, B. I. HALPERIN, AND P. A. LEE, *Ground State of Two-Dimensional Electrons in Strong Magnetic Fields and  $\frac{1}{3}$  Quantized Hall Effect*, Phys. Rev. Lett., **50**, 1219 (1983).